# 1

# AIE or AIEE Materials for Electroluminescence Applications

**Chiao-Wen Lin and Chin-Ti Chen**

*Institute of Chemistry, Academia Sinica, Taiwan*

COPYRIGHTED MATERIAL

## 1.1 Introduction

The science and technology of organic light-emitting diodes (OLEDs) have been developing and progressing for more than 30 years since a small team led by Tang at Kodak invented the first thin-film-based high-efficiency OLED [1]. Nowadays, OLEDs have reached a stage where they are ready to be one of the main types of display in the marketplace, as is evident from the market demand for smartphones and tablets along with Samsung's Galaxy production line of AMOLED mobile devices. Several breakthroughs and discoveries, either intentionally or simply by serendipity, have brought OLEDs beyond being just a research niche in the laboratory. In this chapter, we illustrate one such serendipity, namely the aggregation-induced emission (AIE) or aggregation-induced enhanced emission (AIEE) found for a certain kind of fluorescent materials that leads to an electroluminescence (EL) efficiency of nondopant devices comparable to that of dopant-based OLEDs, the fabrication of which process is more complicated and less easy to control. AIE or AIEE is an inverse effect (see NPAFN and NPAMLI shown in Figure 1.1a) with respect to the more common aggregation-caused quenching (ACQ) or concentration-quenching effect (see Nile Red, DCM1, and TPP shown in Figure 1.1b) that takes place for most fluorophores in the solid state [2]. The difference between AIE and AIEE effects is the relative intensity of the fluorescence [or more generally photoluminescence (PL)] in solution, which is very much solvent dependent. If the chosen solvent enables no or nearly no PL of the material, any PL observed in the solid state is called AIE effect. If solution PL is observed but it is less intense than that in the solid state, the material is sad to show an AIEE effect. Since OLED devices are fabricated in a thin solid film structure, the common ACQ effect impairs the solid-state material PL or EL of OLEDs, the PL quantum yield or the brightness (electroluminance, $L$) of OLEDs, and hence the EL efficiency of OLEDs. Accordingly, materials that display PL having AIE or AIEE characteristics, instead of

*Aggregation-Induced Emission: Applications*, First Edition. Edited by Anjun Qin and Ben Zhong Tang.
© 2013 John Wiley & Sons, Ltd. Published 2013 by John Wiley & Sons, Ltd.

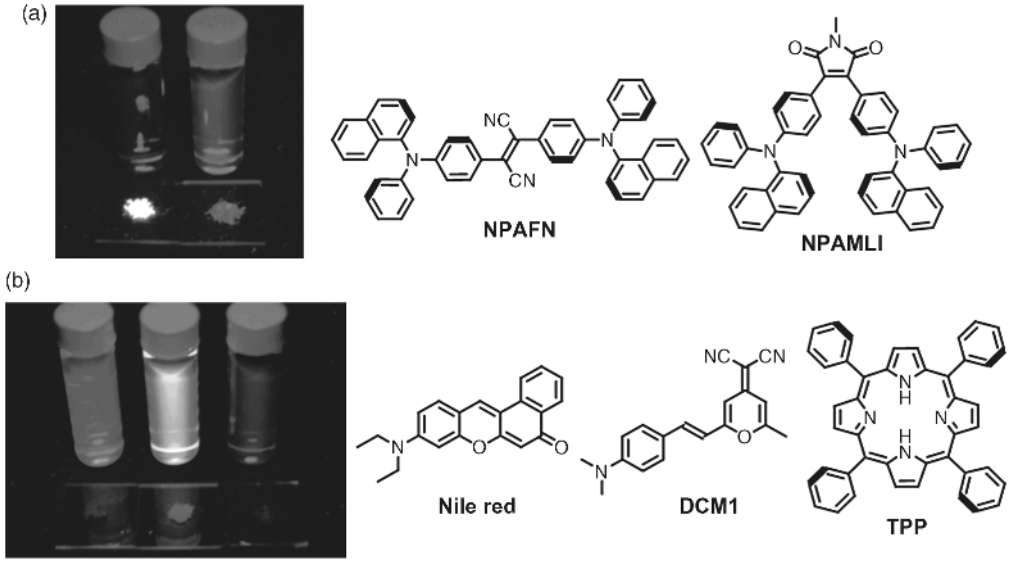


***Figure 1.1*** *From left to right: fluorescence image of (a) NPAFN and NPAMLI and (b) Nile Red, DCM1, and TPP in solution ($CH_2Cl_2$) and in the solid state. Reproduced with permission from [2], © 2004 American Chemical Society.*

ACQ, are very desirable and valuable for high-performance OLEDs fabricated by a simpler fabrication process.

In a survey of the literature, we found many PL materials showing an AIE or AIEE effect but only a few of them have been reported with EL data, that is, their OLEDs were not fabricated and tested. For those have been applied in OLEDs, according to their chemical structure, we classify AIE or AIEE materials into five main categories and an extra category. The first two are five-membered heterocyclic compounds, namely silicon-containing silole derivatives (Section 1.3), imide-containing maleimide derivatives and nitrogen-containing pyrrole derivatives (Section 1.4), the third type is cyano-substituted stilbenoid and distyrylbenzene derivatives (Section 1.5), the fourth type is triarylamine-based derivatives (Section 1.6), and the fifth type is tri- or tetraphenylethene derivatives (Section 1.7). Finally, we group the white OLEDs containing AIE or AIEE materials into an extra category (Section 1.8). Fluorescent materials showing the AIE or AIEE effect are advantageous with respect to the solid-state PL quantum yield, which is one of four key factors that are decisive for achieving high EL efficiency, the external quantum efficiency (EQE or $\eta_{EXT}$), of OLEDs. Therefore, after this introductory section, the chapter begin with the background to EL, EL efficiency, color chromaticity, and fabrication issues of OLEDs. The rest of the chapter considers the six categories of AIE or AIEE molecular materials outlined above.

## 1.2 EL Background, EL Efficiency, Color Chromaticity, and Fabrication Issues of OLEDs

A typical architecture of an OLED device is illustrated in Figure 1.2. The diode device is composed of two electrodes, anode and cathode, sandwiching a hole-transporting layer (HTL), light-emitting layer (EML), and electron-transporting layer (ETL) at the center.

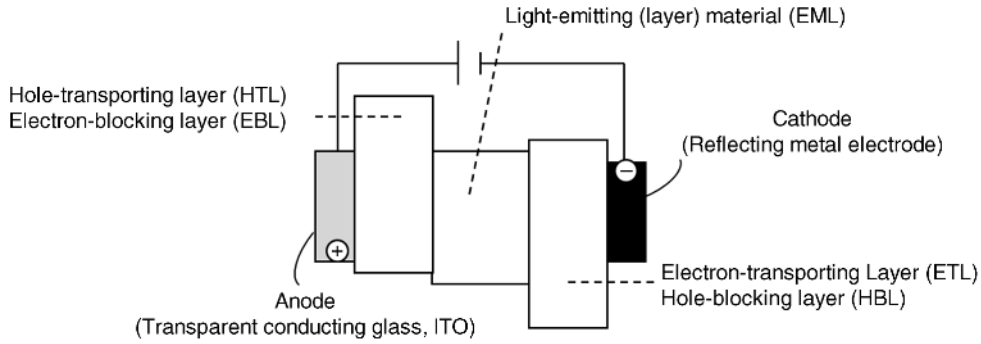


***Figure 1.2*** *Typical architecture of an OLED device. ITO, indium tin oxide.*

The anode is usually transparent, enabling EL from the device, and it is usually an indium tin oxide (ITO)-coated glass substrate. For the cathode, low work function metals, such as Al and Ca, or a metal alloy, such as Mg–Ag, are common choices. To facilitate charge injection and reduction of the driving voltage, injection layers are sometimes inserted adjacent to the electrodes. For electron injection, inorganic ionic substance such as LiF, CsF, or $Cs_2CO_3$ and low work function metal such as Ba or Cs are commonly adopted as the electron injection layer (EIL) in OLED fabrication. Owing to the usually <5.0 eV ionization potential or work function of ITO, materials having a shallow highest occupied molecular orbital (HOMO) energy level or work function are necessary for the hole injection layer (HIL) in OLED fabrication. Scheme 1.1 summarizes HIL materials mentioned in this chapter.

For charge transport and hence charge balance in OLEDs, materials for the hole-transporting layer (HTL) and electron-transporting layer (ETL) are needed in OLED fabrication. HTL materials usually have a high-lying HOMO energy level and a relatively high hole mobility, such as the commonly used TPD and NPB shown in Scheme 1.2.

If the stability of OLED operation is the primary concern, TFTPA HTL will be a better choice than TPB or NPB because of its high glass transition temperature ($T_g$) of more than 185 °C [3]. If wide bandgap HTL materials are necessary, compounds such as CDBP and TCTA are used for phosphorescence-based OLEDs. For ETL of OLEDs, an electron-deficient nature of the molecular structure and relatively low-lying lowest unoccupied molecular orbital (LUMO) level are a common feature of the materials used, such as $Alq_3$,

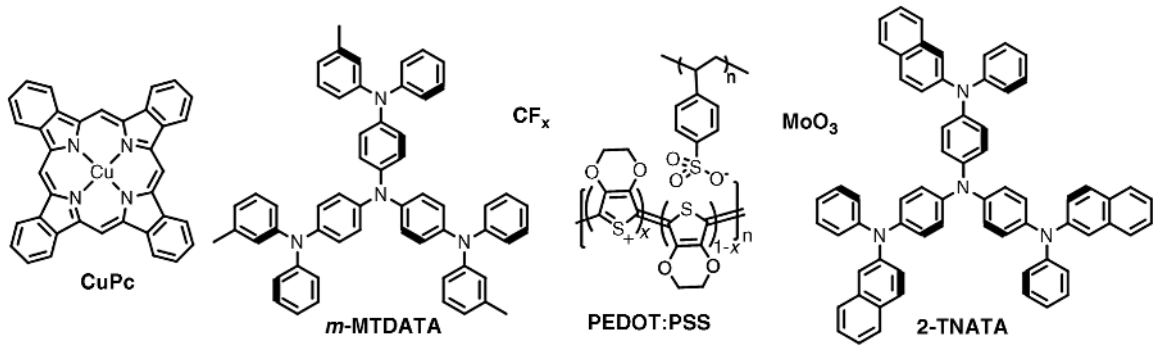


***Scheme 1.1*** *HIL materials mentioned in this chapter.*

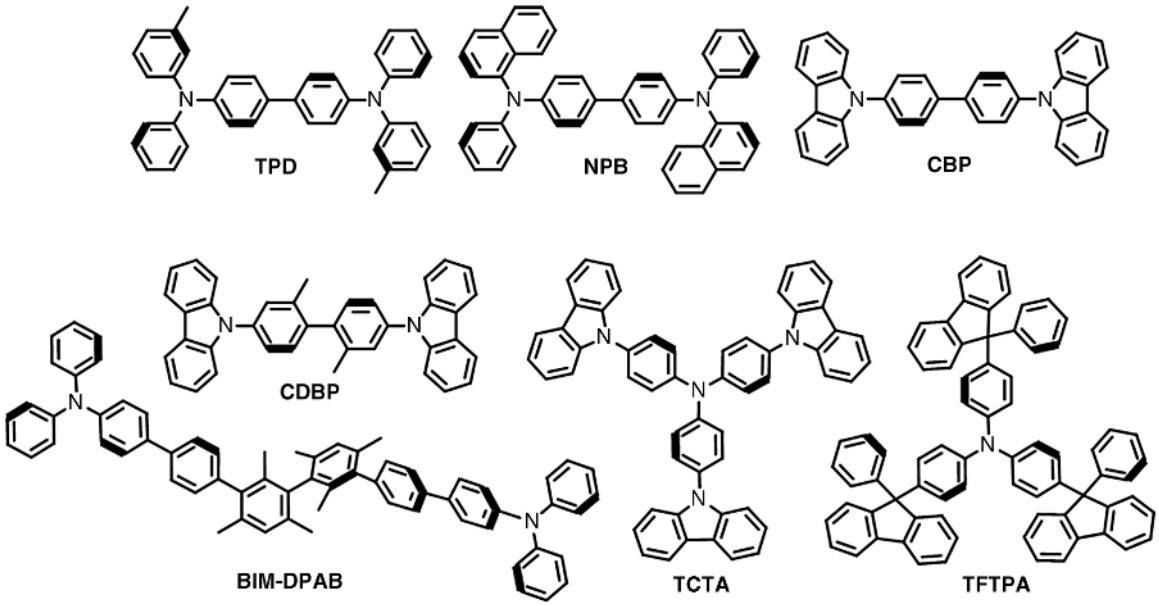


***Scheme 1.2*** *HTL materials mentioned in the chapter.*

PyPySPyPy, TPBI, TAZ, BCP, and BPhen shown in Scheme 1.3. If the ETL material has a particularly low-lying HOMO energy level, such as >6.5 eV as for BCP and BPhen, it is useful for the hole-blocking layer (HBL) between the light-emitting layer (EML) and ETL to confine or enhance the charge recombination on EML.

Using the charge balance factor ($\gamma$), the partition ratio of emissive states ($r_{ST}$), that is, exciton in singlet or triplet state (25 or 75%), PL quantum yield ($\eta_{PL}$), and the light out-coupling efficiency ($\xi$), the basic equation for EQE or $\eta_{EXT}$ of the OLED can be written as [4]

$$\eta_{EXT} = \gamma r_{ST} \eta_{PL} \xi \tag{1.1}$$

Figure 1.3 depicts schematically each factor or component in Equation 1.1.

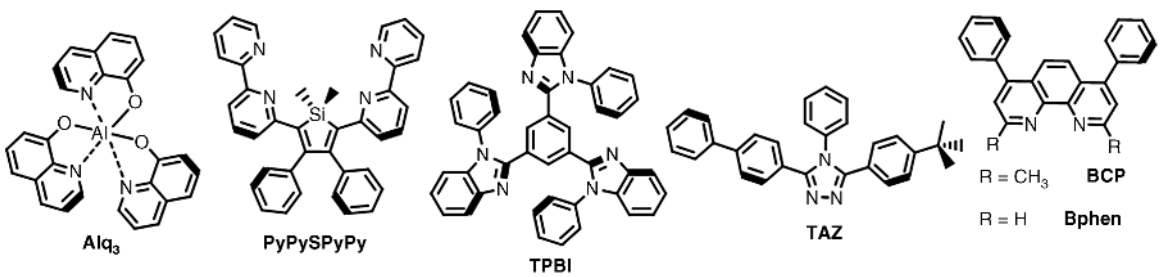


***Scheme 1.3*** *ETL materials mentioned in the chapter.*

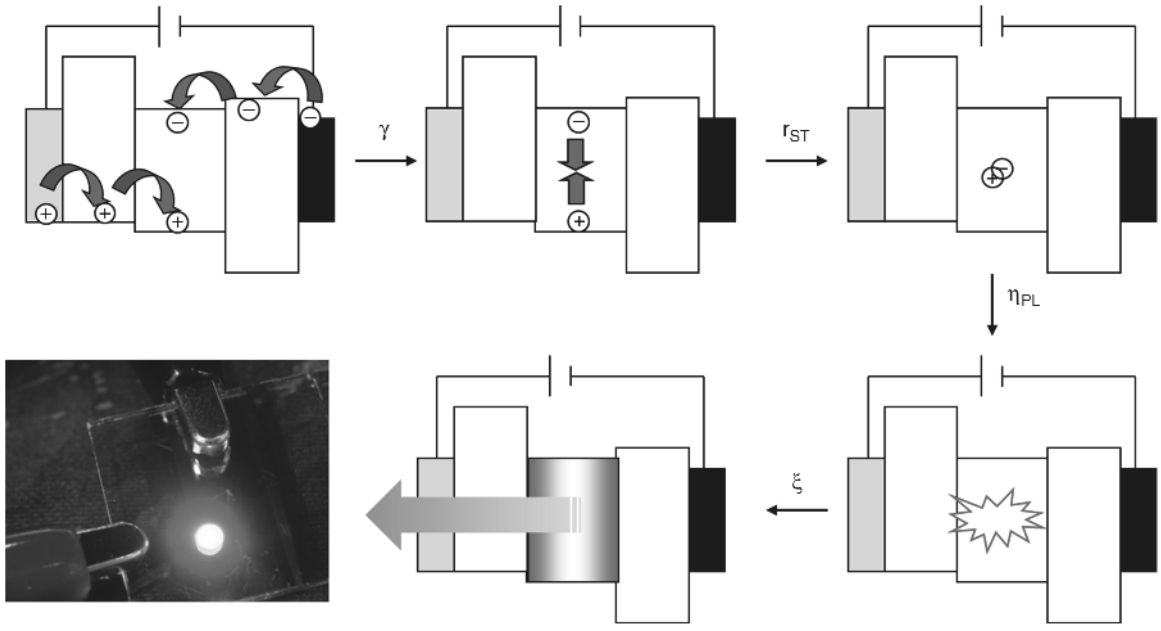


***Figure 1.3*** *Schematic depiction of each term ($\gamma$, $r_{ST}$, $\eta_{PL}$, $\xi$) in Equation 1.1. A photograph of a turn-on red light-emitting OLED is included for illustration purposes.*

Whereas the charge balance ($\gamma$) depends on the charge carrier mobility and energy level alignment of each material in an OLED device, the solid-state PL quantum yield ($\eta_{PL}$) is directly related to the AIE or AIEE effect of the material. The theoretical maximum $\eta_{EXT}$ that one OLED can achieve depends on the light out-coupling ($\xi$) of the device and the nature of the emitting light ($r_{ST}$), either fluorescence or phosphorescence or both, of the materials used in OLEDs. For the first approximation, $\xi$ is proportional to $1/(2n^2)$, where $n$ is the refractive index of the light-emitting layer and is commonly in the range 1.5–1.7 for most PL and EL materials. Accordingly, $\xi \approx 0.17$–$0.22$ and $\eta_{EXT} \sim 20\%$ is the theoretical prediction of the maximum $\eta_{EXT}$. In fact, by utilizing both the phosphorescence and fluorescence energy in OLEDs, $\eta_{EXT}$ values beyond theoretical limit and approaching 30% have been realized [5–7.] Even for OLEDs showing only fluorescence-based EL, $\eta_{EXT} \approx 5\%$, the top limit predicted by theory, has also been exceeded. One of the highest $\eta_{EXT}$ values of $\sim 8\%$ for a fluorescence-based OLED was reported with EML using silole compounds [8], the fluorescent materials showing AIE. Incidentally, two other commonly used units for EL efficiency are $\mathrm{cd\,m^{-2}}$ for the current efficiency ($\eta_C$) and $\mathrm{lm\,W^{-1}}$ for power efficiency ($\eta_P$).

As mentioned earlier, particularly in the solid state, light-emitting materials showing the AIE or AIEE effect can directly contribute to the high $\eta_{PL}$, which is beneficial for promoting the brightness ($L$, electroluminance) and $\eta_{EXT}$ of the OLED. Whereas it is irrelevant to $r_{ST}$ or $\xi$ in Equation 1.1, light-emitting materials showing the AIE or AIEE effect do not necessarily have a high $\gamma$. Therefore, there are numerous OLEDs that show decent to exceptionally good $\eta_{EXT}$ values, but there are even more OLEDs that show poor $\eta_{EXT}$, even though the device contains AIE or AIEE materials as the EML.

Before moving on to the next section, the PL or EL color specification is worth noting here. The RGB color specification is one of the quality checks for full-color OLED displays. Figure 1.4 shows a typical standardized 1931 CIE (Commission Internationale de l'Eclairage) color chromaticity diagram [9].

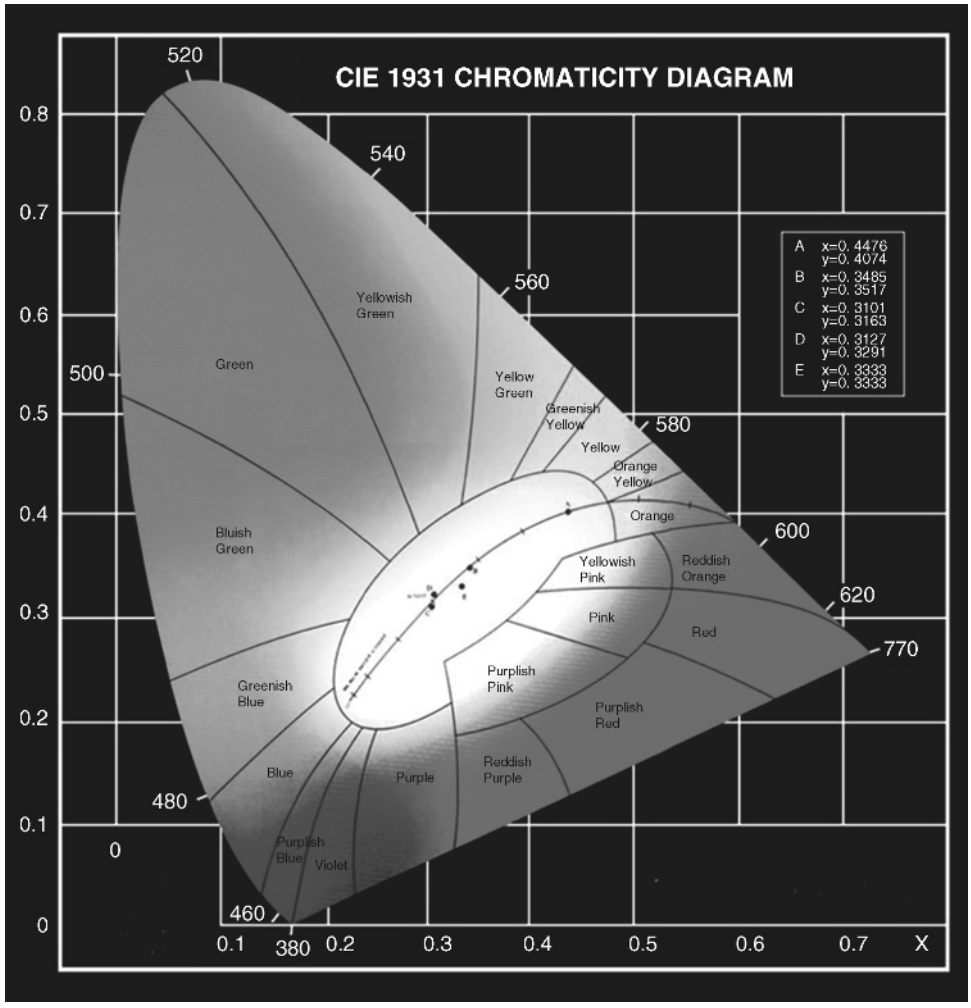


***Figure 1.4*** *A typical 1931 CIE color chromaticity diagram [9].*

Considering the wide color gamut range of a display, it is highly desirable that the materials used in an OLED display should exhibit a color purity of red, green, or blue that is as high as possible. This issue is a challenge to be overcome particularly for blue and red. Moreover, the problems associated with blue and red light-emitting material differ. It is relatively difficult to acquire pure or deep blue-emitting material because of the red-shifting emission, either PL or EL, caused by material aggregation in the solid state, which applies also to AIE or AIEE materials. For red light-emitting materials, red-shifted PL or EL is satisfactory in terms of red color purity. It is the emission intensity that is usually impaired due to the material aggregation in the solid state, which is most serious for red light-emitting materials [2]. However, the AIE or AIEE effect of red light-emitting materials can alleviate the problem of reduced emission intensity. Moreover, in

order to reduce the adverse ACQ of light-emitting materials, OLED fabrication often utilizes a doping process. Unfortunately, this fabrication process is relatively problematic in terms of uniformity and reproducibility, thus hindering a high production yield in volume fabrication [2]. AIE or AIEE materials can take advantage of a 'nondoping process' in OLED fabrication and hence are more feasible for volume production of OLED devices.

Finally, for white OLEDs (WOLEDs) in lighting applications, the EL efficiency under lighting conditions ($L \geq 1000\,\mathrm{cd\,m^{-2}}$) should be examined, because most of the OLED devices exhibit efficiency 'roll-off' at high brightness, and most exhibit peak or maximum EL efficiency ($\eta_{EXT}$, $\eta_C$, or $\eta_P$) at low current density or low brightness. Such low brightness may be acceptable for small-sized displays (such as those on smartphones or the display panel of laptop computers), but is insufficient for lighting applications. In addition, for lighting applications, the color rendering index (CRI) is an important specification of WOLEDs. The CRI is a quantitative measure of the ability of a light source to reproduce the colors of various objects faithfully in comparison with an ideal or natural light source, that is, sunlight. A CRI of 100 represents the maximum value, which is defined for sunlight. An incandescent lamp is a poor light source because of its low efficiency, but it has an excellent CRI of >95, almost as high as for sunlight. A light source with CRI >80 is usually required for general lighting applications. Normally, a two-color-white light source rarely has CRI >80 and a three-color white light system is necessary to achieve CRI >80 for practical lighting applications.

## 1.3 AIE or AIEE Silole Derivatives for OLEDs

The first literature report on OLEDs based on a series of silole-based small-molecule compounds, DMTPS, MPClTPS, MPTPS, and HPS (Table 1.1) as EML, by Tang *et al.*, appeared in 2001 [10]. The performance of the OLEDs was rather poor (maximum brightness $L_{max} < 5000\,\mathrm{cd\,m^{-2}}$ and $\eta_{EXT} < 1\%$). At about the same time, one of the silole compounds, MPTPS (known as MPS in the literature), was also reported separately with significantly improved OLEDs performance ($L_{max} > 9200\,\mathrm{cd\,m^{-2}}$, $\eta_{EXT} = 8\%$, $\eta_C = 12$, $\eta_P = 12.6$ or $20\,\mathrm{lm\,W^{-1}}$) [11]. In this paper [11], the specific term 'aggregation-induced emission' (AIE) was mentioned for the first time to manifest the extraordinary behavior of the solid-state fluorescence. The OLED data for MPTPS were elaborated further in a paper published in 2002 [8]. Basically, the super high $\eta_{EXT}$ value (8%) beyond ~5.5%, the theoretical limit of fluorescence-based EML, is attributed to the underestimated $\xi$ and $r_{ST}$. Also in 2002, another silole-based AIE material, 2PSP, was employed as the EML in OLEDs by Kafafi and co-workers, with $\eta_{EXT}$ as high as 4.8% and $\eta_P$ as high as $12\,\mathrm{lm\,W^{-1}}$, which ranks the second highest in Table 1.1, next to MPTPS [12]. The high $\eta_{EXT}$ of the reported MPTPS and 2PSP OLEDs may also be ascribed to the high electron mobility of the silole compound, such as PyPySPyPy shown in Scheme 1.3. Its electron mobility was determined $2 \times 10^{-4}\,\mathrm{cm^2\,V^{-1}\,s^{-1}}$, which is more than two orders of magnitude higher than that of the most widely used electron transport material, tris(8-hydroxyquinolinolato)aluminum(III) ($Alq_3$) [13].

Not matching the needs of display applications, all silole-based AIE or AIEE materials listed in Table 1.1 show EL with less desirable colors: greenish blue, green, yellowish green, and even yellow (DPyASPTPS). There seems to be one plausible exception, $HPS_{2,4}$, for which an OLED exhibited EL with $\lambda_{max}^{EL} = 464\,\mathrm{nm}$ and a reasonably good $\eta_C$ of $5.86\,\mathrm{cd\,A^{-1}}$ has been reported (see Table 1.1) [16]. However, there is no information available regarding the 1931 $CIE_{x,y}$ color chromaticity of the device. Based on the EL spectrum displayed in the paper, the $HPS_{2,4}$ OLED exhibits a fairly wide EL band [the full width-at-half-maximum (FWHM) is >100 nm] and such an EL band has substantial intensity (more than one-third of the peak intensity at $\lambda_{max}^{EL} = 464\,\mathrm{nm}$) extending far beyond 550 nm. Even though EL peaked at a relatively short wavelength of 464 nm, the color of the $HPS_{2,4}$ OLED is

***Table 1.1*** *Summary of reported OLEDs containing silole-based AIE or AIEE materials.*

| AIE or AIEE fluorophore | $\lambda_{max}^{EL}$, $CIE_{x,y}$, color code (nm), (*x*, *y*), color | $V_{on}$ (V) | $L_{max}$ (cd $m^{-2}$) | $\eta_{EXT}$ (%) | $\eta_C$ (cd $A^{-1}$) | $\eta_P$ (lm $W^{-1}$) | Ref. |
|---|---|---|---|---|---|---|---|
| EML | ITO/TPD/EML/$Alq_3$/Al | | | | | | 10 |
| DMTPS | 494 (–, –) green–blue | 9 | 222 | 0.03 | – | – | |
| MPClTPS | 494 (–,–) green–blue | 7 | 23 | 0.01 | – | – | |
| MPTPS | 494 (–, –) green–blue | 11 | 4538 | 0.65 | – | – | |
| HPS | 488 (–, –) green–blue | 12 | 1188 | 0.31 | – | – | |
| MPTPS | TO/CuPc/TPD/MPTPS/$Alq_3$/LiF/Al | | | | | | 11 |
| | 496 (–, –) green–blue | 3.4 | 9234 | 8 | 12 | 12.6 | |
| 2PSP | ITO/TPD/2PSP/PyPySPyPy/Mg:Ag | | | | | | 12 |
| | 500 (–, –) green–blue | 2.5 | 1400 | 4.8 | – | 12 | |
| MPTPS | ITO/CuPc/TPD/MPTPS/$Alq_3$/LiF/Al | | | | | | 8 |
| | 490 (–, –) green–blue | – | >10000 | 8 | 20 | 14 | |
| EML | ITO/NPB/EML/PyPySPyPy/Mg:Ag | | | | | | 14 |
| 2PSP | 495 (–, –) green–blue | ~3 | >10000 | 3.8 | – | 4.6 | |
| ASP | 525 (–, –) green | ~2.3 | >7000 | 3.8 | – | 5.2 | |
| PPSPP | 500~(–, –) green–blue | ~3.3 | >7000 | 3.4 | – | 4.0 | |
| EML | ITO/TPD/EML/PyPySPyPy/Mg:Ag | | | | | | |
| 2PSP | 495 (–, –) green–blue | ~2.6 | >10000 | 4.1 | – | 8.5 | |
| ASP | 525 (–, –) green | –2.3 | >7000 | 4.0 | – | 9.6 | |
| HPS | ITO/CuPc/TPD/HPS/$Alq_3$/LiF/Al | | | | | | 15 |
| | 497 (–, –) green–blue | 4 | 55880 | 7 | 15 | 10 | |
| $HPS_{2,4}$ | ITO/NPB/$HPS_{2,4}$/$Alq_3$/LiF/Al | | | | | | 16 |
| | 464 (–, –) green–blue | – | 2250 | – | 5.86 | – | |
| DPyASPTPS | ITO/NPB/DPyASPTPS/LiF/Al | | | | | | 17 |
| | 566 (–, –) yellow | 3.2 | 8440 | – | <2.5 | – | |
| | ITO/DPyASPTPS/LiF/Al | | | | | | |
| | 557 (–, –) yellow | 3.8 | 48 | – | – | – | |
| EML | ITO/NPB/EML/TPBI/$Alq_3$/LiF/Al | | | | | | 18 |
| DMTPS-CHO | 516 (0.33, 0.47) yellow–green | 11.3 | 322 | 0.05 | 0.13 | 0.03 | |
| DMTPS-DCV | 548 (0.38, 0.53) yellow–green | 5.7 | 210 | 0.01 | 0.02 | 0.01 | |
| DMTPS-DPA | 544 (0.39, 0.53) yellow–green | 3.1 | 13405 | 2.42 | 8.28 | 7.88 | |
| DMTPS-DPA | ITO/NPB/DMTPS-DPA/TAZ/$Alq_3$/LiF/Al | | | | | | |
| | 544 (0.38, 0.59) yellow–green | 4.3 | 7886 | 0.10 | 3.35 | 2.19 | |
| DMTPS-DPA | ITO/DMTPS-DPA/TPBI/$Alq_3$/LiF/Al | | | | | | |
| | 548 (0.40, 0.57) yellow–green | 3.1 | 14038 | 2.26 | 7.60 | 6.94 | |
| EML | ITO/NPB/EML/TPBI/LiF/Al | | | | | | 19 |
| D-1-NpTPS | 512 (–, –) blue–green | 4.7 | 15700 | 1.6 | 4.9 | 1.8 | |
| D-2-NpTPS | 536 (–, –) green | 4.4 | 9420 | 3.2 | 10.5 | 7.3 | |

***Table 1.1*** *(Continued).*

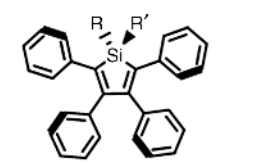


| | | |
|---|---|---|
| $R = CH_3$ | $R' = CH_3$ | **DMTPS** |
| $CH_3$ | $(CH_2)_3Cl$ | **MPCITPS** |
| $CH_3$ | Ph | **MPTPS** |
| Ph | Ph | **HPS** |

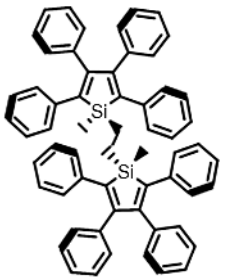


**2PSP**

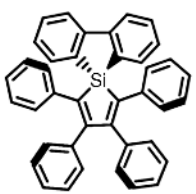


**ASP**

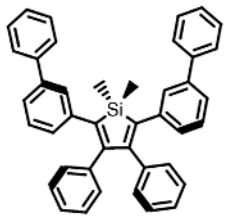


**PPSPP**

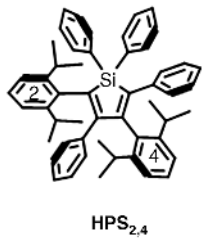


**$HPS_{2,4}$**

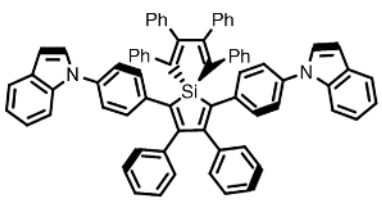


**INSPTPS**

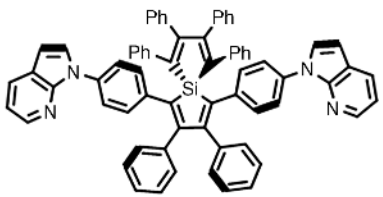


**AZINSPTPS**

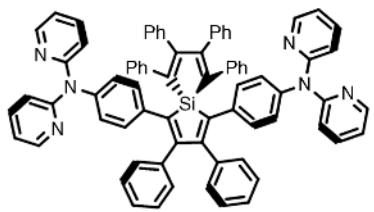


**DPyASPTPS**

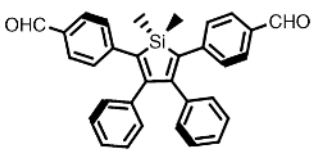


**DMTPS-ALD**

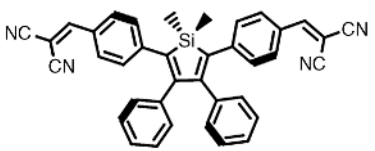


**DMTPS-DCV**

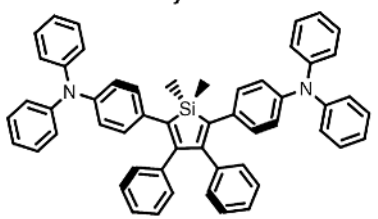


**DMTPS-DPA**

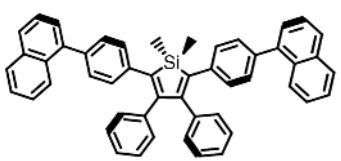


**D-1-NpTPS**

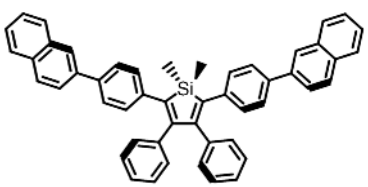


**D-2-NpTPS**

unlikely to be authentic blue and more possibly green–blue or blue–green as for most silole-based AIE or AIEE materials. The silole $HPS_{2,4}$ has built-in steric hindrance due to the isopropyl substituent at the *ortho*-position of two phenyl rings forcing a twist on the π-conjugation and shortening the EL wavelength. Based on fundamental intuition, the twisted conformation should be helpful in reducing the exciplex formation with the HTL (such as TPB and NPB), which usually results in a red-shifted emission wavelength. Therefore, the higher than normal EL intensity around 550 nm may be partly due to $Alq_3$, the material used as the ETL in an $HPS_{2,4}$ OLED.

## 1.4 AIE or AIEE Maleimide and Pyrrole Derivatives for OLEDs

In 2002, Chen and co-workers reported a red OLED based on NPAMLI, a maleimide fluorophore, as the EML in a nondopant device [20], namely a red OLED fabricated without the application of a doping process. This is one of the first long-wavelength (>600 nm) AIE or AIEE materials to be reported for OLED application and yet the OLED exhibited reasonably good performance. The NPAMLI OLED exhibited $L_{max} \approx 8000\,cd\,m^{-2}$ and $\eta_{EXT} = 2.4\%$ (Table 1.2), and such a performance is comparable to that of red OLEDs fabricated with a doping process.

It is worth mentioning that the device was fabricated without an HTL because NPAMLI has the capability of transporting holes in an OLED. NPAMLI shares a common structural feature, namely 2-naphthylphenylamine, with NPB (Scheme 1.2), one of the most widely used materials for HTLs. In fact, when the paper was first published it was not realized that the maleimide NPAMLI is indeed one of the materials that show an AIE or AIEE effect. The image shown in Figure 1.1a demonstrating the AIEE effect (dichloromethane solution versus solid state) was taken two years later in 2004. To provide the missing evidence thus far, Figure 1.5 displays the AIE effect of NPAMLI in acetonitrile solution with increasing amount of water addition (from left to right).

***Figure 1.5*** *Fluorescence images of NPAMLI in acetonitrile–water mixture with water fractions of 0, 20, 50, 60, 70, and 80% from left to right.*

***Table 1.2*** *Summary of reported OLEDs containing maleimide- or pyrrole-based AIE or AIEE materials.*

| AIE or AIEE fluorophore | $\lambda_{max}^{EL}$, $CIE_{x,y}$, color code (nm), (*x*, *y*), color | $V_{on}$ (V) | $L_{max}$ (cd m$^{-2}$) | $\eta_{EXT}$ (%) | $\eta_C$ (cd A$^{-1}$) | $\eta_P$ (lm W$^{-1}$) | Ref. |
|---|---|---|---|---|---|---|---|
| NPAMLI | ITO/NPAMLI/BCP/TPBI/Mg:Ag | | | | | | 20 |
| | 650 (0.66, 0.32) orange–red | 3.3 | ~8000 | 2.4 | 1.5 | 0.9 | |
| NPAMLI (*x*, *y*) | ITO/NPB(*x* nm)/NPAMLI (*y* nm)/$Alq_3$/Mg:Ag | | | | | | 21 |
| 40, 10 | 646 (0.45, 0.47) yellow | – | 10360 | 1.5 | – | – | |
| 20, 30 | 650 (0.48, 0.46) yellow | – | 8050 | 1.2 | – | – | |
| 5, 50 | 524 (0.38, 0.50) yellow–green | – | 17910 | 1.1 | – | – | |
| NPAMLI (*x*, *y*, *z*) | ITO/NPB (*x* nm)/NPAMLI (*y* nm)/BCP(*z* nm)/$Alq_3$/Mg:Ag | | | | | | |
| 40, 10, 5 | 648 (0.61, 0.37) red–orange | 3.5 | 5180 | 0.9 | – | – | |
| 20, 30, 5 | 646 (0.63, 0.35) red–orange | 3.6 | 4320 | 0.9 | – | – | |
| 5, 30, 20 | 652 (0.67, 0.33) red | 4 | 3920 | 1.6 | – | – | |
| NPAMLI (*x*, *y*, *z*) | ITO/NPAMLI (*x* nm)/BCP(*y* nm)/$Alq_3$/Mg:Ag | | | | | | |
| 50, 5, – | 650 (0.65, 0.34) orange–red | 3.8 | 4570 | 0.8 | – | – | |
| 50, 10, – | 650 (0.65, 0.33) orange–red | 3.5 | 3585 | 1.4 | – | – | |
| EML | ITO/NPB/EML/$Alq_3$/Mg:Ag | | | | | | 22 |
| INMLI1 | 526, 600 (0.38, 0.50) yellow–green | 4.0 | 10400 | 0.42 | – | – | |
| INMLI1F | 522 (0.33, 0.54) green | 3.7 | 14800 | 0.76 | – | – | |
| INMLI2 | 526 (0.39, 0.50) yellow–green | 3.7 | 10500 | 0.39 | – | – | |
| INMLI2F | 530 (0.39, 0.52) yellow–green | 3.7 | 16800 | 0.71 | – | – | |
| INMLI3 | 530 (0.42, 0.50) green–yellow | 3.3 | 11400 | 0.63 | – | – | |
| INMLI3F | 600 (0.50, 0.45) yellow | 4.0 | 6800 | 0.40 | – | – | |
| INMLI4F | 520 (0.33, 0.54) green | 3.0 | 13000 | 0.57 | – | – | |
| EML | ITO/NPB/EML/TPBI/Mg:Ag | | | | | | |
| INMLI1 | 636 (0.63, 0.36) red–orange | 4.1 | 2710 | 0.34 | – | – | |
| INMLI1F | 390, 638 (0.50, 0.28) pink | 4.6 | 2780 | 0.45 | – | – | |
| INMLI2 | 390, 630 (0.61, 0.37) red–orange | 4.1 | 2700 | 0.32 | – | – | |
| INMLI2F | 410, 630 (0.60, 0.37) red–orange | 3.9 | 2800 | 0.38 | – | – | |
| INMLI3 | 410, 612 (0.58, 0.39) orange | 3.4 | 5400 | 0.55 | – | – | |
| INMLI3F | 420, 602 (0.52, 0.38) orange yellow | 3.8 | 4600 | 0.50 | – | – | |
| INMLI4F | 410, 660 (0.42, 0.32) orange white | 4.0 | 1030 | 0.25 | – | – | |
| NPANPy | ITO/NPANPy/$Alq_3$/LiF/Al | | | | | | 23 |
| | 525 (0.29, 0.57) green | 2.5 | 43226 | 1.69 | 5.58 | 4.77 | |
| | ITO/NPANPy/TPBI/LiF/Al | | | | | | |
| | 458 (0.16, 0.14) blue | 3.0 | 3602 | 1.45 | 1.48 | 0.62 | |
| | ITO/NPB/NPANPy/$Alq_3$/LiF/Al | | | | | | |
| | 524 (0.30, 0.56) green | 2.5 | 49505 | 1.82 | 5.95 | 6.46 | |

(*continued*)

***Table 1.2*** (*Continued*)

| AIE or AIEE fluorophore | $\lambda_{max}^{EL}$, $CIE_{x,y}$, color code (nm), (*x*, *y*), color | $V_{on}$ (V) | $L_{max}$ (cd m$^{-2}$) | $\eta_{EXT}$ (%) | $\eta_C$ (cd A$^{-1}$) | $\eta_P$ (lm W$^{-1}$) | Ref. |
|---|---|---|---|---|---|---|---|
| | ITO/NPB/NPANPy/TPBI/LiF/Al | | | | | | |
| | 460 (0.16, 0.17) blue | 3.0 | 4748 | 1.37 | 1.68 | 1.14 | |
| AsINMLIa | ITO/*m*-MTDATA/NPB/AsINMLIa/BCP/$Alq_3$/LiF/Al | | | | | | 24 |
| | 615 (0.61, 0.39) red–orange | 6.0 | 3950 | 0.48 | 0.80 | 0.17 | |
| EML | ITO/NPB/EML/TPBI/LiF/Al | | | | | | |
| AsINMLIc | 615 (0.59, 0.41) orange | 5.0 | 6040 | 0.67 | 1.11 | 0.31 | |
| AsINMLId | 615 (–, –) orange | 4.5 | 6605 | 0.59 | 0.85 | 0.23 | |
| AsINMLIe | 615 (–, –) orange | 4.5 | 5612 | 0.46 | 0.70 | 0.23 | |
| AsINMLIf | 615 (–, –) orange | 4.0 | 9750 | 1.06 | 1.07 | 0.40 | |
| | ITO/NPB/EML/BCP/$Alq_3$/LiF/Al | | | | | | |
| AsINMLIb | 615 (–, –) orange | 4.5 | 5618 | 0.60 | 0.87 | 0.24 | |
| AsINMLId | 615 (–, –) orange | 4.5 | 7794 | 0.72 | 1.05 | 0.30 | |
| AsINMLIe | 615 (–, –) orange | 4.5 | 5976 | 0.54 | 0.83 | 0.29 | |
| AsINMLIf | 628 (–, –) red–orange | 4.0 | 7634 | 1.08 | 1.09 | 0.30 | |

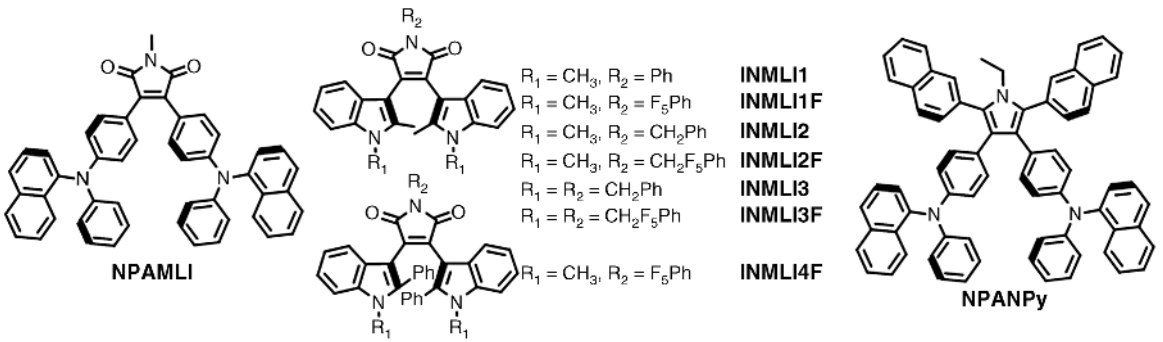


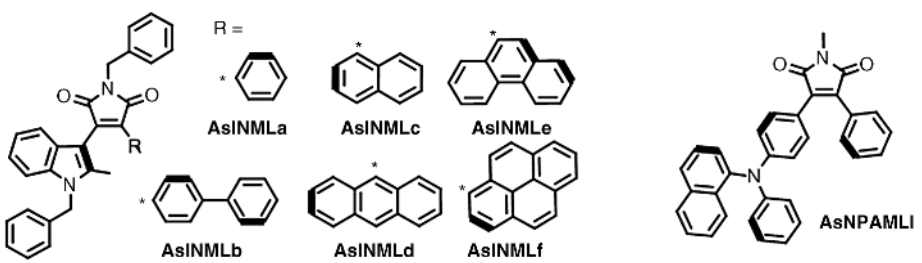

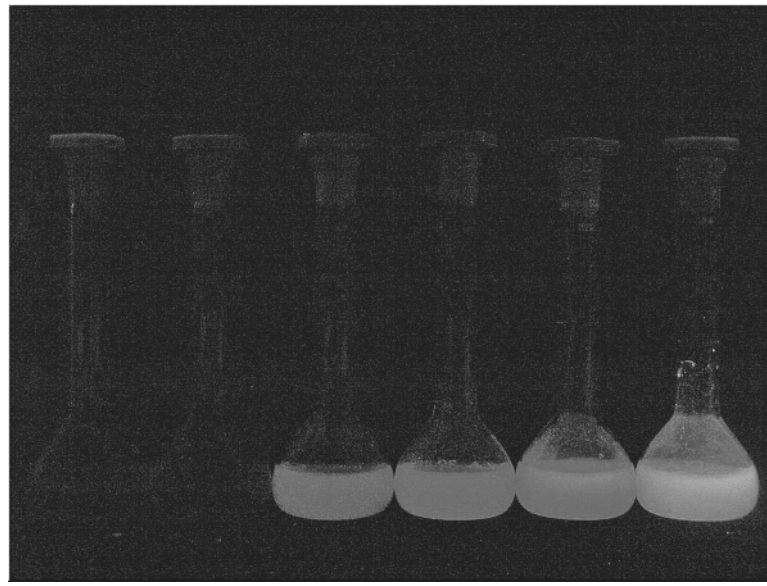

***Figure 1.6*** *Fluorescence images of AsNPAMLI in acetonitrile–water mixture with water fractions of 0, 20, 50, 60, 70, and 80% from left to right. (See color figure in color plate section).*

Recently, our laboratory synthesized an asymmetric NPAMLI, the red–orange AsNPAMLI (see Table 1.2 for its structure). Although its OLED application awaits exploration, we have clearly demonstrated its AIE effect in solution (Figure 1.6).

More maleimide compounds bearing indole substituents (Table 1.2), either symmetrical (INMLI series) or asymmetric (AsINMLI series) [22, 24], were subsequently reported for OLED application. However, all of these indole-substituted maleimide OLEDs show shorter EL wavelengths in the orange to red–orange region and their performances are all inferior to that of the first reported NPAMLI OLED.

One non-maleimide-based material listed in Table 1.2 is a five-membered heterocylic pyrrole derivative, NPANPy [23]. Pyrroles are nitrogen-containing five-membered cyclic dienes similar to siloles except that the silicon is the heteroatom of the five-membered ring structure. Structure-wise, tetraaryl-substituted pyrrole derivatives have a propeller-like molecular conformation very similar to that of tetraaryl-substituted silole derivatives. Recent studies have revealed that a propeller-like molecular structure is vital for the AIE or AIEE effect caused by the restriction of intramolecular bond rotation in the solid state. It is not surprising that such pyrrole derivatives exhibit stronger fluorescence intensities than those in dichloromethane solution [23], a typical AIEE effect found for structurally similar silole derivatives. Unlike the electron-deficient nature of the silole derivatives, pyrrole derivatives are electron rich and seldom produce red-shifted exciplex emission with the HTL. Therefore, it is relatively easy for pyrrole derivatives to achieve blue EL when fabricated as the EML in OLEDs. Provided that low-lying HOMO TPBI is used as the ETL, authentic blue EL with 1931 $CIE_{x,y}$ (0.16, 0.14–0.17) can be readily obtained (Table 1.2). However, the EL efficiency is not very good (none of the $\eta_{EXT}$ values of the blue emissions is more than 1.5%).

## 1.5 AIE or AIEE Cyano-Substituted Stilbenoid and Distyrylbenzene Derivatives for OLEDs

The observation of the enhanced fluorescence on cyano-substituted stilbenoid and distyrylbenzene derivatives (CN-DSB) in the solid state can be traced back as early as that of silole derivatives. In fact, one of the first reported CN-DSB OLEDs was observed in 2002 by Luo *et al.* [25]. However, the device was fabricated with CN-DSB*x* (Table 1.3) by a doping process and the reported OLED performance was far from satisfactory. Shortly after, in 2003, Chen and co-workers reported high performance (maximum $\eta_{EXT} \approx 2.4\%$) nondopant red–orange OLEDs containing a dicyano-substituted, 2-naphthylphenylamine-appended stilbenoid, NPAFN (Table 1.3) [26]. Once again, similarly to the case of the NPAMLI OLED, NPAFN OLEDs performed better without including NPB as the HTL. As shown in Figure 1.1a, NPAFN exhibits a pronounced AIE or AIEE effect. The AIE or AIEE effect of NPAFN has recently been confirmed in solution, as shown in Figure 1.7.

Several years later, in 2008, Chen and co-workers developed the second generation of NPAFN, PhSPFN and FPhSPFN (Table 1.3) [27]. With longer π-conjugation between donor and acceptor moieties, PhSPFN and FPhSPFN OLEDs both display EL at longer wavelength, corresponding to authentic red color chromaticity, 1931 $CIE_{x,y}$ (0.67, 0.30) and (0.66, 0.34), respectively. The maximum $\eta_{EXT}$ of the FPhSPFN OLED reaches 3.1%, one of the highest among AIE or AIEE nondopant red OLEDs, only exceeded by TTPEBTTD [maximum $\eta_{EXT} = 3.7\%$, $CIE_{x,y}$ (0.67, 0.32)] [28]. In this case, AIE and AIEE take place for PhSPFN and FPhSPFN, respectively (Figure 1.8). The fluorine *ortho*-substituent of FPhSPFN enhances the restriction of intramolecular bond rotation and hence increases the fluorescence intensity not only in the solid state but also in solution.

***Figure 1.7*** *Fluorescence images of NPAFN in acetonitrile–water mixture with water fractions of 0, 20, 50, 60, 70, and 80% from left to right.*

***Table 1.3*** *Summary of reported OLEDs containing cyano-substituted stilbenoid and distyrylbenzene AIE or AIEE materials.*

| AIE or AIEE fluorophore | $\lambda_{max}^{EL}$, $CIE_{x,y}$, color code (nm), (*x*, *y*), color | $V_{on}$ (V) | $L_{max}$ (cd $m^{-2}$) | $\eta_{EXT}$ (%) | $\eta_C$ (cd $A^{-1}$) | $\eta_P$ (lm $W^{-1}$) | Ref. |
|---|---|---|---|---|---|---|---|
| CN-DSB*x* | ITO/NPB/CBP/TPBI:CN-DSB*x*/TPBI/Mg:Ag | | | | | | 25 |
| CN-DSB$_o$ | 494 (0.16, 0.40) blue–green | 5.5 | 6695 | 0.51 | – | – | |
| CN-DSB$_m$ | 516 (0.26, 0.61) green | 6.5 | 6499 | 1.70 | – | – | |
| CN-DSB$_p$ | 518 (0.29, 0.61) green | 6.0 | 9321 | 0.78 | – | – | |
| NPAFN | ITO/NPAFN/BCP/TPBI/Mg:Ag | | | | | | 26 |
| | 634 (0.64, 0.36) red–orange | 3.6 | 9359 | 2.4 | 2.5 | 1.7 | |
| | ITO/NPB/NPAFN/BCP/TPBI/Mg:Ag | | | | | | |
| | 636 (0.64, 0.36) red–orange | 3.4 | 10034 | 1.8 | 2.0 | 0.9 | |
| PhSPFN | ITO/NPB/PhSPFN/BCP/TPBI/LiF/Al | | | | | | 27 |
| | 674 (0.67, 0.30) red | 3.8 | 2600 | 1.8 | – | – | |
| FPhSPFN | ITO/NPB/FPhSPFN/BCP/TPBI/LiF/Al | | | | | | |
| | 642 (0.66, 0.34) red | 4.0 | 10100 | 3.1 | – | – | |
| 2-NPAFN | ITO/NPB/2-NPAFN/BCP/TPBI/LiF/Al | | | | | | 29 |
| | 666 (–, –) red | 6.1 | 1420 | – | 1.34 | 0.42 | |
| | ITO/2-NPAFN/BCP/TPBI/LiF/Al | | | | | | |
| | 664 (–, –) red | 8 | 650 | – | 0.81 | 0.05 | |
| EFPAFN | ITO/NPB/EFPAFN/BCP/TPBI/LiF/Al | | | | | | |
| | 677 (–, –) red | 5.9 | 3370 | – | 2.27 | 0.75 | |
| | ITO/EFPAFN/BCP/TPBI/LiF/Al | | | | | | |
| | 680 (–, –) red | 8.4 | 1290 | – | 0.51 | 0.06 | |
| CN-DPASDB | ITO/NPB/CN-DPASDB/TPBI/LiF/Al | | | | | | 30 |
| | 579 (0.50, 0.50) yellow | 5 | 14667 | | 4.0 | | |
| CN-DPABS | ITO/$CF_x$/CN-DPABS/TPBI/LiF/Al | | | | | | 31 |
| | 644 (0.61, 0.38) red–orange | 10.2 | ∼900 | 0.77 | 0.67 | 0.22 | |
| CN-PhzBS | ITO/$CF_x$/CN-PhzBS/TPBI/LiF/Al | | | | | | |
| | 568 (0.46, 0.50) green–yellow | 9.53 | ∼900 | 0.33 | 0.83 | 0.25 | |

(*continued*)

***Table 1.3*** (*Continued*)

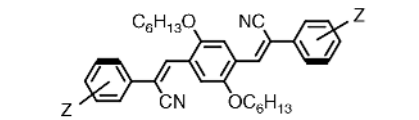


Z = *ortho*-$OCH_3$ Z = *meta*-$OCH_3$ Z = *para*-$OCH_3$

**CN-DSB*o*** **CN-DSB*m*** **CN-DSB*p***

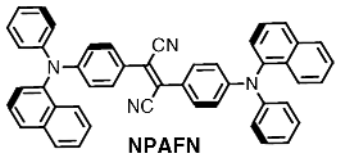


**NPAFN**

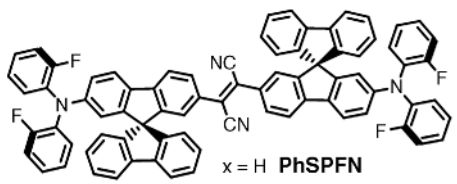


x = H **PhSPFN**

x = F **FPhSPFN**

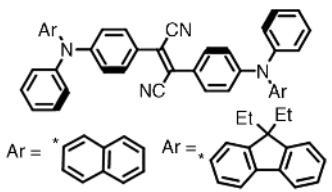





**β-NPAFN**




**FlPAFN**

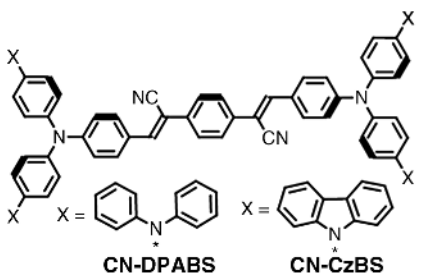


**CN-DPABS** **CN-CzBS**

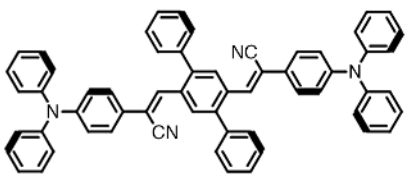


**CN-DPASDB**

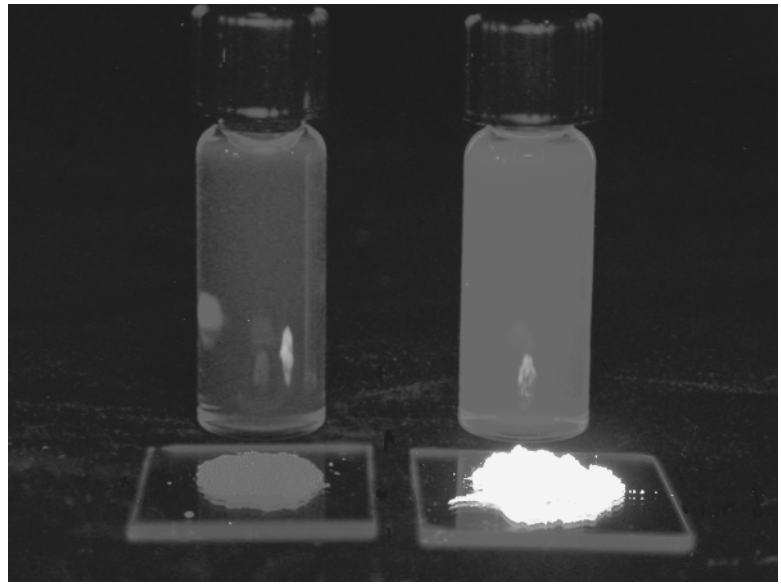

***Figure 1.8*** *Fluorescence images of PhSPFN (a) and FPhSPFN (b) in solution (dichloromethane) and in the solid state. (See color figure in color plate section).*

Although EFPAFN in Table 1.3 has a longer EL wavelength and hence better chromaticity of red color, in terms of EL efficiency [29], FPhSPFN is by far one of the best red AIE or AIEE materials for OLED application. In Table 1.3, CN-DPASDB exhibits a fairly high $\eta_C$ of 4.0 cd $A^{-1}$ but it is a yellow OLED [31], mostly not a desirable color for display applications.

## 1.6 AIE or AIEE Triarylamine Derivatives for OLEDs

Triarylamines represent the smallest family of AIE or AIEE materials, although they are often present in the molecular structure of long wavelength-emitting AIE or AIEE materials (see examples in Section 1.4 and Section 1.5). A triarylamine has an electron-rich character and is therefore suitable as a strong electron donor in structural design, readily raising the HOMO energy level and narrowing the emission bandgap energy of the molecular compound. Basically, a triarylamine molecule possesses a nonplanar molecular structure, similar to the propeller-like structural feature of most AIE or AIEE materials. Two types of triarylamine-based AIE or AIEE materials have been demonstrated for OLED application (Table 1.4). Constructed with an appropriate electron acceptor segment, two of them (SBCN and M1) exhibit near-IR emission [32, 33], although their OLED performance is rather poor, not very different from those of other near-IR OLEDs reported in the literature.

## 1.7 AIE or AIEE Triphenylethene and Tetraphenylethene Derivatives for OLEDs

As summarized in this section, a wide variety of chemical structures have been reported for tri- and tetraphenylethene derivatives. This group of organic fluorophores is one of the latest discovered AIE or AIEE

***Table 1.4*** *Summary of reported OLEDs containing triarylamine-based AIE or AIEE materials.*

| AIE or AIEE fluorophore | $\lambda_{max}^{EL}$, $CIE_{x,y}$, color code (nm), ($x$, $y$), color | $V_{on}$ (V) | $L_{max}$ (cd m$^{-2}$) | $\eta_{EXT}$ (%) | $\eta_C$ (cd A$^{-1}$) | $\eta_P$ (lm W$^{-1}$) | Ref. |
|---|---|---|---|---|---|---|---|
| EML | ITO/PEDOT:PSS/EML/TPBI/Ba/Al | | | | | | 32 |
| CZCHO | 505 (–, –) green–blue | 7.2 | 804 | 2.09 | 3.03 | – | |
| SBCHO | 542 (–, –) green | 9.3 | 330 | 1.33 | 1.13 | – | |
| CZCN | 644 (–, –) red–orange | 11.6 | 111 | 0.61 | 0.30 | – | |
| SBCN | 724 (–, –) near-IR | 8.6 | 55 | 0.05 | 0.03 | – | |
| EML | ITO/EML/TPBI/Ba/Al | | | | | | |
| CZCN | 646 (–, –) red–orange | 10.9 | 140 | 0.93 | 0.47 | – | |
| SBCN | 724 (–, –) near-IR | 8.6 | 69 | 0.05 | 0.02 | | |
| M1 | ITO/$MoO_3$/NPB/M1/BCP/$Alq_3$/LiF/Al | | | | | | 33 |
| | 1050 (–, –) near-IR | 5 | 60[a] | 0.05 | – | – | |
| | ITO/$MoO_3$/NPB/M1/TPBI/LiF/Al | | | | | | |
| | 1050 (–, –) near-IR | – | – | ∼0 | – | – | |

[a]In units of W Sr$^{-1}$ m$^{-2}$.

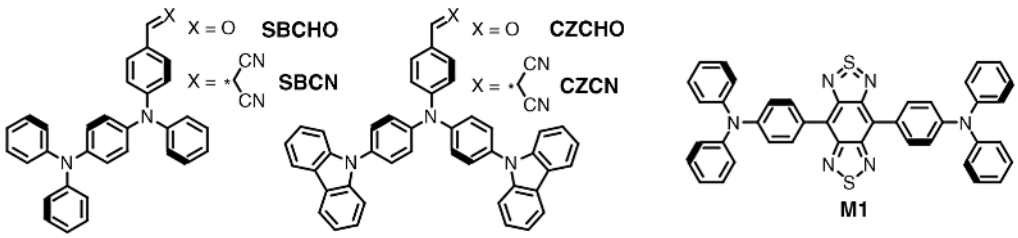


materials, although this family is the largest in number. However, their OLED application was documented long before the invention of AIE or AIEE terminology.

The first compound considered in this section is DPVBi (Table 1.5), which was first commercialized by Idemitsu Kosan Co. as one of the most widely used blue fluorophores in the mid-1990s [34]. Apart from being a derivative of triphenylethene, DPVBi can also be looked as upon as a diphenyl-substituted stilbenoid dimer. In fact, the tetraphenylethene moiety can also be considered as a cross-conjugated stilbenoid. The triphenylethene moiety exhibits a similar propeller shape of to the tetraphenylethene moiety. As illustrated by other examples shown in Section 1.5, stilbenoid compounds are well known for the free rotor effect on the radiationless transitions that cause serious fluorescence quenching in solution state [35, 36].

The AIE or AIEE effect of DPVBi has never been shown until now (see Figure 1.9). Accordingly, in terms of the AIE or AIEE effect and structural similarity, triphenylethene derivatives can be considered as one member of the large tetraphenylethene family. According to our survey, the best nondopant DPVBi OLED was probably reported by Park and co-workers in 2007 (Table 1.5) [41]. The device was fabricated as a control OLED and it was an authentic blue device with an EL wavelength at 465 nm corresponding to 1931 $CIE_{x,y}$ (0.15, 0.16). The device has a maximum $\eta_C$ of 3.92 cd A$^{-1}$ and a maximum $\eta_P$ of 1.61 lm W$^{-1}$, which are good compared with other OLEDs in Table 1.6 having a similar blue color purity.

In addition to the early work on DPVBi, triphenylethene and tetraphenylethene have been attached to anthracene (Table 1.5), one of the first organic fluorophores studied for EL by Pope et al. in the 1960s [45].

***Table 1.5*** *Summary of reported OLEDs containing DPVBI, DPVPA, or TPVAn AIE or AIEE materials.*

| AIE or AIEE fluorophore | $\lambda_{max}^{EL}$, $CIE_{x,y}$, color code (nm), (*x*, *y*), color | $V_{on}$ (V) | $L_{max}$ (cd $m^{-2}$) | $\eta_{EXT}$ (%) | $\eta_C$ (cd $A^{-1}$) | $\eta_P$ (lm $W^{-1}$) | Ref. |
|---|---|---|---|---|---|---|---|
| DPVBi | ITO/CuPc/TPD/DPVBi/$Alq_3$/Mg:Ag | | | | | | 34 |
| | 480 (–, –) green–blue | – | 6000 | – | 2 | – | |
| | ITO/TPD/DPVBi/$Alq_3$/LiF/Al | | | | | | 37 |
| | 476 (–, –) green–blue | <4 | 3000 | 1.4 | – | 0.64 | |
| | ITO/CuPc/NPB/DPVBi/$Alq_3$/CsF/Al | | | | | | 38 |
| | 460 (0.15, 0.15) blue | – | – | 3.5 | – | 1.0 | |
| | ITO/NPB/DPVBi/$Alq_3$/LiF/Al | | | | | | 39 |
| | 456 (0.16, 0.14) blue | <4 | 2107 | – | 1.78 | 1.10 | |
| | ITO/TPD/DPVBi/BCP/LiF/Al | | | | | | 40 |
| | 452, 479 (0.16, 0.21) blue | <4 | – | ~2.5 | | | |
| | ITO/2-TNATA/NPB/DPVBi/$Alq_3$/LiF/Al | | | | | | 41 |
| | 465 (0.15, 0.16) blue | – | – | – | 3.92 | 1.61 | |
| | ITO/NPB/DPVBi/TPBI/LiF/Al | | | | | | 42 |
| | 468 (0.15, 0.08) deep blue | 5.0 | 4828 | 2.3 | 1.7 | 0.93 | |
| DPVPA | ITO/$CF_x$/NPB/DPVPA/$Alq_3$/LiF/Al | | | | | | 43 |
| | –- (0.14, 0.17) blue | – | – | 3 | 1.4 | 0.7 | |
| TPVAn | ITO/NPB/TPVAn/TPBI/Mg:Ag | | | | | | 44 |
| | 454 (0.15, 0.11) blue | 3.9 | 5500 | 3.1 | 3.1 | 1.5 | |
| | ITO/TFTPA/TPVAn/TPBI/Mg:Ag | | | | | | |
| | 454 (0.14, 0.11) blue | 3.4 | 6400 | 4.1 | 4.1 | 2.1 | |
| | ITO/PEDOT/TFTPA/TPVAn/TPBI/Mg:Ag | | | | | | |
| | 456 (0.14, 0.12) blue | 4.9 | 6700 | 5.3 | 5.3 | 2.8 | |
| EML | ITO/2-TNATA/NPB/EML/$Alq_3$/LiF/Al | | | | | | 40 |
| BTBPPA | 463 (0.165, 0.195) blue | – | – | – | 5.03 | 1.67 | |
| BTPPA | 452 (0.159, 0.160) blue | – | – | – | 3.93 | 1.82 | |

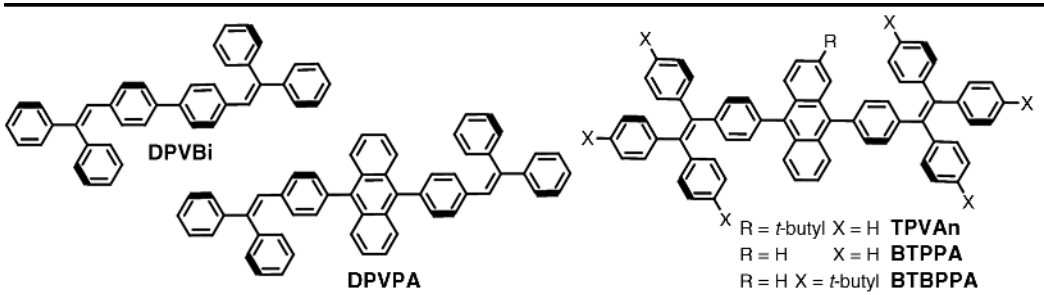

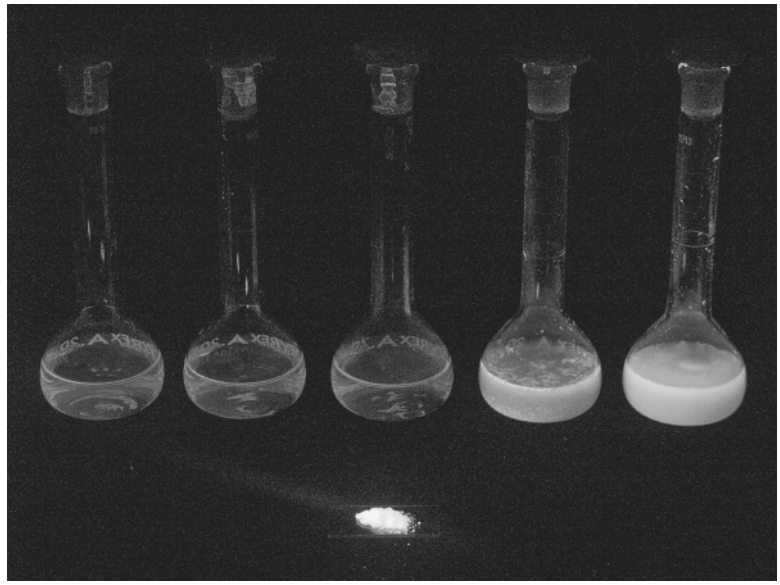

***Figure 1.9*** *Fluorescence images of DPVBi in THF–water mixture with water fraction 0, 20, 40, 60, and 80% from left to right. Its solid-state fluorescence image is shown in front of the solution samples. (See color figure in color plate section).*

***Table 1.6*** *Summary of reported OLEDs containing DPFv-$NH_2$, DPFV-OMe, TPE, TPEPh, BTPE, or TDPVBi AIE or AIEE materials.*

| AIE or AIEE fluorophore | $\lambda_{max}^{EL}$, $CIE_{x,y}$, color code (nm), (*x*, *y*), color | $V_{on}$ (V) | $L_{max}$ (cd $m^{-2}$) | $\eta_{EXT}$ (%) | $\eta_C$ (cd $A^{-1}$) | $\eta_P$ (lm $W^{-1}$) | Ref. |
|---|---|---|---|---|---|---|---|
| EML | ITO/NPB/EML/BCP/$Alq_3$/LiF/Al | | | | | | 47 |
| DPFv-$NH_2$ | ~485 (–, –) green–blue | – | 5000 | – | 1.90 | 0.7 | |
| DPFv-OMe | 520 (–, –) green | – | 449 | – | – | – | |
| EML | ITO/NPB/EML/BCP/$Alq_3$/LiF/Al | | | | | | 48 |
| TPE | 445 (–, –) deep blue | 2.9 | 1800 | 0.4 | 0.45 | 0.35 | |
| TPEPh | 476 (–, –) green–blue | 5 | 10680 | 2.56 | 5.15 | – | |
| BTPE | ITO/NPB/BTPE/TPBI/$Alq_3$/LiF/Al | | | | | | 49 |
| | 488 (–, –) green–blue | 4 | 11180 | 3.17 | 7.26 | 3.81 | |
| TDPVBi | ITO/NPB/TDPVBi/TPBI/LiF/Al | | | | | | 42 |
| | 468 (0.16, 0.21) blue | 3.8 | 31170 | 3.8 | 6.2 | 3.94 | |

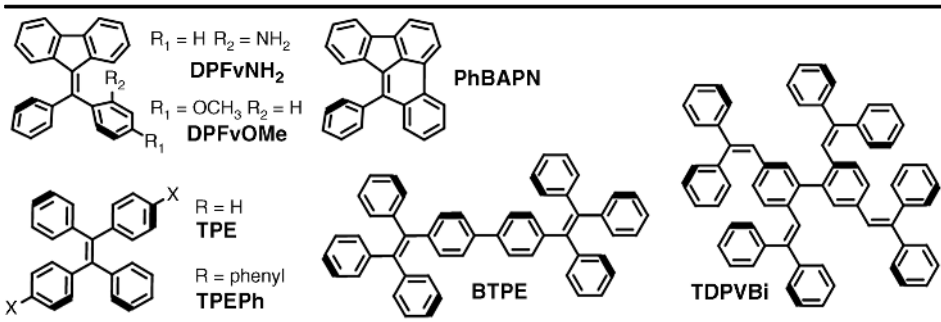

DPVPA is bistriphenylethene-attached anthracene [43] and TPVAn, BTPPA, and BTBPPA are bistetraphenylethene-attached anthracene derivatives [41, 44]. Among all the compounds listed in Table 1.6, the nondopant TPVAn OLED shows the highest fluorescence-based EL efficiency ($\eta_{EXT} = 5.3\%$). In addition, its blue color purity is excellent, 1931 $CIE_{x,y}$ (0.14, 0.12), corresponding to an authentic blue color. This is not surprising because the solution PL quantum efficiency of 9,10-diphenylanthracene is very high and close to unity [46]. The bulky propeller-like tetraphenylethene substituent prevents the anthracene moiety from close contact and red shifting the emission wavelength. On the other hand, bistetraphenylethene substituents contribute to the strong AIE or AIEE effect that simply preserves the high PL quantum efficiency of the material in the solid state.

$DPFvNH_2$ and $DPFvNH_2$ are two-ring-fused versions of tetraphenylethene, although the propeller molecular shape remains and the AIE or AIEE effect is observed [47]. $DPFvNH_2$ and $DPFvNH_2$ OLEDs have been fabricated and tested, and the results were not very good (Table 1.6). Both devices have a significantly red-shifted EL at 485 and 520 nm, respectively, and weak EL has been observed for $DPFvNH_2$ OLEDs, Considering the red-shifted and weak EL, it can be suspected that $DPFvNH_2$ forms an excimer in the thin-film device. Interestingly, PhBAPN is a three-ring-fused version of tetrephenylethene and the propeller-like structure of $DPFvNH_2$ and $DPFvNH_2$ no longer exists in this compound (Table 1.6), so nor is the AIE or AIEE effect. A PhBAPN OLED was reported with an even weaker excimer EL ($L_{max} = 219\,cd\,m^{-2}$) at 556 and 580 nm [47].

Whereas TPE is the parent structure of tetraphenylethene, TPEPh is probably the simplest tetraphenylethene derivative (Table 1.6) [48], being a single phenyl-substituted TPE. In the literature, the solid-state PL wavelength of TPEPh was demonstrated to be morphology dependent. It is 454 and 503 nm for crystalline and amorphous TPEPh, respectively, although its EL wavelength is at 476 nm and it is green–blue. The EL efficiency of green–blue TPEPh is just moderate ($\eta_{EXT} = 2.56\%$, $\eta_C = 5.15\,cd\,A^{-1}$). The parent compound TPE has a very short EL wavelength at 445 nm (indicative of a deep blue color) and nearly overlaps with the PL spectrum of its crystal. However, the device's $L_{max}$ is only $\sim 1800\,cd\,m^{-2}$ and none of the EL efficiency criteria is over 0.5 (%, $cd\,A^{-1}$, or $lm\,W^{-1}$), although a very low turn-on voltage ($L$ of the device equal to $1\,cd\,m^{-1}$) of 2.9 V was observed for a TPE OLED.

BTPE is a single covalent bond-connected dimer form of the parent TPE structure (Table 1.6) [49]. Like TPE or TPEPh mentioned above, BTPE is one of the tetraphenylethene derivatives having a relatively simple chemical structure. Its solid-state PL also behaves similarly to TPEPh, with the PL wavelength being morphology dependent, 445 and 499 nm for crystalline fibers and amorphous film, respectively. Similarly to a TPEPh OLED, the BTPE EL wavelength at 488 nm (green–blue) is between the PL wavelengths of crystalline and amorphous samples, although its OLED performance is better than that of TPEPh OLEDs. On the other hand, TDPVBi can be considered as a triphenylethene version of BTPE bearing two extra propeller-like moieties (Table 1.6) [42]. It also can be considered as an 'upgraded' version of DPVBi because of the two extra propeller-like moieties. Concerning the OLED performance, TDPVBi has a much shorter EL wavelength at 468 nm corresponding to a green–blue color, 1931 $CIE_{x,y}$ (0.16, 0.21), which is bluer than that of the TPEPh OLED. The EL efficiency of the TDPVBi OLEDs is also in general better than that of TPEPh OLEDs.

$TPESiPh_3$, $(TPE)_3SiPh_2$, and $(TPE)_2SiPh$ are hybrid structures of TPE and tetraphenylsilane (Table 1.7) [50], which is known for the amorphous feature of the OLED material that can extend the morphological stability of the thin-film structure in OLEDs [51, 52]. However, from the reported OLED data for these materials, as more TPE units are attached to the tetraphenylsilane, the performance of the OLEDs becomes worse, not only the EL efficiency and maximum brightness but also the EL wavelength (becoming longer with less blue color purity). Among the series, the least TPE-containing $TPESiPh_3$ has the best-performing OLED. It is an authentic blue OLED with a short EL wavelength at 452 nm and $L_{max} = 5672\,cd\,cm^{-2}$, but its EL efficiency is not poor ($\eta_{EXT} = 1.6\%$, $\eta_C = 2.1\,cd\,A^{-1}$, $\eta_P = 1.1\,lm\,W^{-1}$).

***Table 1.7*** *Summary of reported OLEDs containing silane-based $TPESiPh_3$, $(TPE)_2SiPh_2$, $(TPE)_3SiPh$ AIE or AIEE materials.*

| AIE or AIEE fluorophore | $\lambda_{max}^{EL}$, $CIE_{x,y}$, color code (nm), (*x*, *y*), color | $V_{on}$ (V) | $L_{max}$ (cd $m^{-2}$) | $\eta_{EXT}$ (%) | $\eta_C$ (cd $A^{-1}$) | $\eta_P$ (lm $W^{-1}$) | Ref. |
|---|---|---|---|---|---|---|---|
| EML | ITO/NPB/EML/TPBI/LiF/Al | | | | | | 50 |
| $TPESiPh_3$ | 452 (–, –) blue | 5 | 5672 | 1.6 | 2.1 | 1.1 | |
| $(TPE)_2SiPh_2$ | 472 (–, –) green–blue | 8 | 3635 | 0.7 | 1.4 | 0.4 | |
| $(TPE)_3SiPh$ | 484 (–, –) green–blue | 7 | 1081 | 0.8 | 1.6 | 0.47 | |

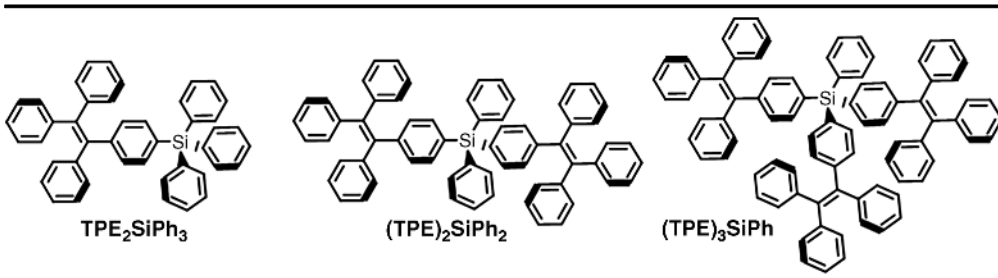


$TPE_2SiPh_3$ $(TPE)_2SiPh_2$ $(TPE)_3SiPh$

In contrast to an earlier report on triarylamine-based AIE or AIEE materials by He and co-workers [42], Tang et al. clearly showed that triphenylamine (TPA) and $N^4,N^4,N^{4'},N^{4'}$-tetraphenylbiphenyl-4,4′-diamine, a TPA dimer (DTPA), are ACQ materials instead of AIE or AIEE materials (Table 1.8) [53]. After attaching three TPE units to TPA or four TPE units to DTPA, 3TPETPA and 4TPEDTPA become typical AIE or AIEE materials. However, regarding their OLEDs, 3TPETPA peculiarly exhibits multiple EL bands at 493 and 511 nm (in a device containing NPB as HTL) or 499 and 513 nm (in a device without NPB HTL), which are both red shifted from PL wavelength in solution (THF–water mixture) of 484 nm. The OLED of 4TPEDTPA behaves normally with a single EL band at 488 nm, which is green–blue not much different from the PL wavelength in solution (THF–water mixture) of 486 nm. Without the red-shifted EL and anomalous emission band, 4TPEDTPA OLEDs outperform 3TPETPA OLEDs.

Pyrene is another fluorophore known for notorious aggregation even in the solution state. Pyrene is a typical ACQ material because of its rigid and flat molecular structure. There have been two approaches to chemical modification of pyrene with a TPE moiety (Table 1.9). The first involves surrounding the pyrene structure with four propeller-like TPE moieties like that of TTPEpy [54]. The second approach is to incorporate pyrene moieties, either one or two, into TPE as part of the structure like those of TPPyE and DPDPyE [55]. Both approaches are successful in changing pyrene from an ACQ material to an AIE or AIEE material. However, considering the performance of the OLEDs, the former approach, namely TTPEpy OLEDs, can reach a high EL efficiency ($\eta_{EXT} = 4.98\%$, $\eta_C = 12.3$ cd $A^{-1}$, $\eta_P = 7.0$ lm $W^{-1}$) and substantially outperforms the latter (TPPyE and DPDPyE). TPPyE and DPDPyE OLEDs are also worse in blue color purity and their EL wavelength is in the range 504–516 nm, which is longer than the 488–492 nm of green-blue TTPEpy OLEDs.

The next group in the triphenylethene family is $DPVP_2Mst$, $DPVPP_2Mst$, and $DPVP_4Mst$ (Table 1.10) [56], which can be considered as an improved version of DPVBi in terms of blue color purity. With two central methyl substituents twisting the biphenyl structure, the effective π-conjugation length of the molecule is reduced, the bandgap energy is increased, and the emission wavelength is shortened. An authentic blue EL, 1931 $CIE_{x,y}$ (0.15, 0.17), was acquired for a $DPVPP_2Mst$ OLED. As the number of triphenylethene

***Table 1.8*** *Summary of reported OLEDs containing triphenylamine-based 3TPETPA or 4TPEDTPA AIE or AIEE materials.*

| AIE or AIEE fluorophore | $\lambda_{max}^{EL}$, $CIE_{x,y}$, color code (nm), (*x*, *y*), color | $V_{on}$ (V) | $L_{max}$ (cd $m^{-2}$) | $\eta_{EXT}$ (%) | $\eta_C$ (cd $A^{-1}$) | $\eta_P$ (lm $W^{-1}$) | Ref. |
|---|---|---|---|---|---|---|---|
| 3TPETPA | ITO/NPB/EML/TPBI/$Alq_3$/LiF/Al | | | | | | 53 |
| | 493, 511 (–, –)green–blue | 5.4 | 1662 | 1.2 | 3.1 | 1.1 | |
| | ITO/EML/TPBI/$Alq_3$/LiF/Al | | | | | | |
| | 499, 513 (–, –)green–blue | 4.5 | 6935 | 1.5 | 4.0 | 1.9 | |
| 4TPEDTPA | ITO/EML/TPBI/$Alq_3$/LiF/Al | | | | | | |
| | 488 (–, –) green–blue | 4.1 | 10723 | 3.7 | 8.0 | 5.2 | |

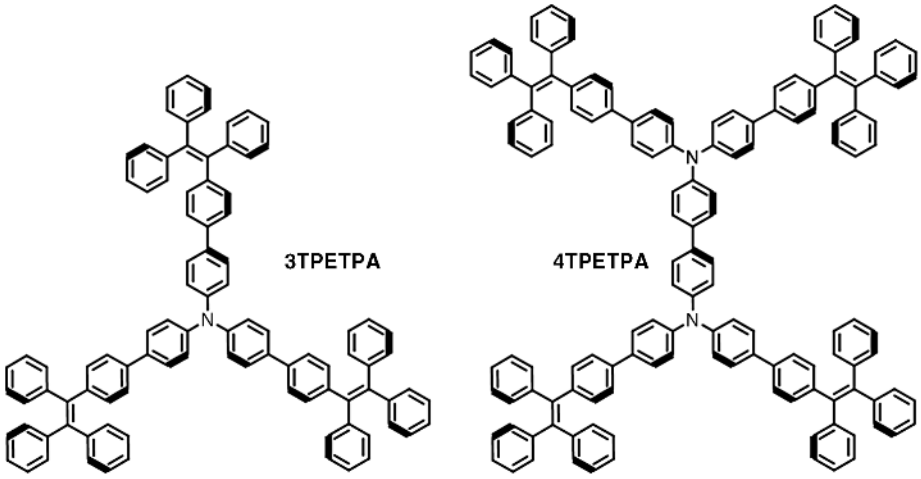


moieties attached increases, the AIE or AIEE effect intensifies the solid-state blue emission of these bimesitylene fluorophores. With Bim-DPAB (Scheme 1.2) as the HTL in the device, the EL efficiency of a $DPVPP_2Mst$ OLED was increased ($\eta_{EXT} = 4.7\%$, $\eta_C = 5.4\,cd\,A^{-1}$, $\eta_P = 2.02\,lm\,W^{-1}$).

The molecular hybrid structure of TPE and silole, two well known AIE or AIEE moieties, seems to be interesting and worth OLED testing. Tang and co-workers prepared 2,5-BTPEMTPS and 3,4-BTPEMTPS after the first failed attempt at the preparation of TPE hybrid hexaphenyl-substituted siloles (Table 1.11) [49]. The silole and TPE hybrids 2,5-BTPEMTPS and 3,4-BTPEMTPS [57] are in fact a pair of structural isomers. Both of their OLEDs exhibit green–yellow EL, that of the 2,5-isomer having a longer wavelength at 552 nm than that of the 3,4-isomer at 520 nm. The not very good performance of nondopant OLEDs can be improved by making a dopant device with BTPE as the host material for 2,5-BTPEMTPS after optimizing the dopant concentration. A similar molecular hybrid approach was applied to TPE and triphenylethene by Chi and co-workers (Table 1.11). [58] One of such hybrid molecules is $(VP)_3$-$(TPE)_3$ and its OLED has been tested. However, $(VP)_3$–$(TPE)_3$ OLEDs perform poorly without EL efficiency data. The device requires a relatively high 6.0 V to be turned on and $L_{max}$ is only 1908 cd $m^{-2}$ Its EL color is not blue but green–blue at 474 nm, corresponding to 1931 $CIE_{x,y}$ (0.18, 0.31).

In order to increase the hole-transporting ability of TPE or triphenylethene AIE or AIEE materials, arylamine moieties are a potent structural feature to be incorporated in the structure [59]. We have seen that 3TPETPA and 4TPEDTPA mentioned earlier (Table 1.8) are two examples following the principle of

***Table 1.9*** *Summary of reported OLEDs containing pyrene-based 3TPETPA or 4TPEDTPA AIE or AIEE materials.*

| AIE or AIEE fluorophore | $\lambda_{max}^{EL}$, $CIE_{x,y}$, color code (nm), ($x$, $y$), color | $V_{on}$ (V) | $L_{max}$ (cd $m^{-2}$) | $\eta_{EXT}$ (%) | $\eta_C$ (cd $A^{-1}$) | $\eta_P$ (lm $W^{-1}$) | Ref. |
|---|---|---|---|---|---|---|---|
| TTPEPy | ITO/NPB/TTPEPy ($x$ nm)/TPBI/LiF/Al | | | | | | 54 |
| 40 nm | 488 (–, –) green–blue | 3.6 | 36300 | 4.95 | 12.3 | 7.0 | |
| 26 nm | 492 (–, –) green–blue | 4.7 | 18000 | 4.04 | 10.6 | 5.0 | |
| EML | ITO/NPB/EML/TPBI/LiF/Al | | | | | | 55 |
| TPPyE | 508 (–, –) blue–green | 4.6 | 15450 | 1.4 | 3.7 | 2.1 | |
| DPDPyE | 520 (–, –) green | 5.3 | 45550 | 2.9 | 9.1 | 4.1 | |
| EML | ITO/NPB/EML/TPBI/$Alq_3$/LiF/Al | | | | | | |
| TPPyE | 504 (–, –) blue–green | 4.6 | 25470 | 2.0 | 4.0 | 2.7 | |
| DPDPyE | 516 (–, –) blue–green | 3.2 | 49830 | 3.3 | 10.2 | 9.2 | |

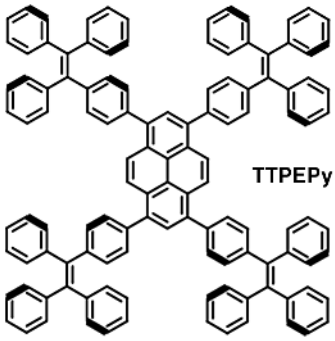


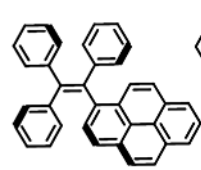


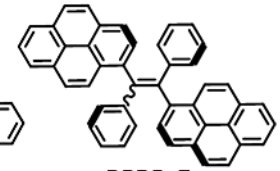


***Table 1.10*** *Summary of reported OLEDs containing bimesitylene-based $DPVP_2Mst$, $DPVPP_2Mst$, or $DPVP_4Mst$ AIE or AIEE materials.*

| AIE or AIEE fluorophore | $\lambda_{max}^{EL}$, $CIE_{x,y}$, color code (nm), ($x$, $y$), color | $V_{on}$ (V) | $L_{max}$ (cd $m^{-2}$) | $\eta_{EXT}$ (%) | $\eta_C$ (cd $A^{-1}$) | $\eta_P$ (lm $W^{-1}$) | Ref. |
|---|---|---|---|---|---|---|---|
| EML | ITO/NPB/EML/BCP/$Alq_3$/LiF/Al | | | | | | 56 |
| $DPVP_2Mst$ | 448 (0.15, 0.09) deep blue | 4.5 | 5415 | 1.52 | 1.22 | 0.55 | |
| $DPVPP_2Mst$ | 462 (0.10, 0.16) blue | 4.5 | 6129 | 1.07 | 1.38 | 0.49 | |
| $DPVP_4Mst$ | 452 (0.16, 0.13) blue | 5.0 | 1466 | 1.06 | 1.15 | 0.39 | |
| EML | ITO/NPB/EML/TPBI/LiF/Al | | | | | | |
| $DPVP_2Mst$ | 452 (0.14, 0.08) deep blue | 4.5 | 4575 | 1.51 | 1.29 | 0.66 | |
| $DPVPP_2Mst$ | 452 (0.14, 0.11) blue | 4.5 | 9031 | 1.95 | 1.80 | 0.95 | |
| $DPVP_4Mst$ | 452 (0.15, 0.12) blue | 5.5 | 1727 | 1.08 | 1.07 | 0.43 | |
| EML | ITO/NPB/CBP/EML/TPBI/LiF/Al | | | | | | |
| $DPVP_2Mst$ | 450 (0.15, 0.10) deep blue | 5.0 | 7599 | 2.12 | 1.90 | 0.93 | |
| $DPVPP_2Mst$ | 456 (0.15, 0.13) blue | 5.0 | 9500 | 2.11 | 2.24 | 1.10 | |
| $DPVPP_2Mst$ | ITO/Bim-DPAB/$DPVPP_2Mst$/TPBI/LiF/Al | | | | | | |
| | 460 (0.15, 0.17) blue | 4.5 | 15361 | 4.70 | 5.40 | 2.02 | |

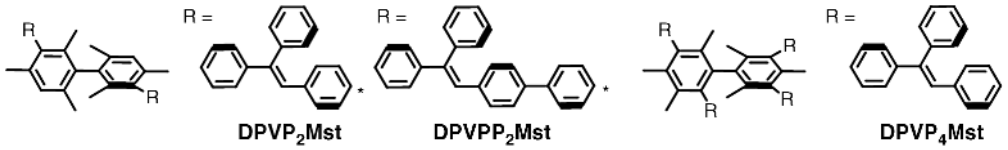

***Table 1.11*** *Summary of reported OLEDs containing TPE–silole hybrid 3,4-BTPEMTPS or 2,5-BTPEMTPS AIE or AIEE materials.*

| AIE or AIEE fluorophore | $\lambda_{max}^{EL}$, $CIE_{x,y}$, color code (nm), ($x$, $y$), color | $V_{on}$ (V) | $L_{max}$ (cd $m^{-2}$) | $\eta_{EXT}$ (%) | $\eta_C$ (cd $A^{-1}$) | $\eta_P$ (lm $W^{-1}$) | Ref. |
|---|---|---|---|---|---|---|---|
| EML | ITO/NPB/EML/TPBI/LiF/Al | | | | | | 57 |
| 3,4-BTPEMTPS | 520 (–, –) green | 6.2 | 3980 | 1.66 | 4.96 | 2.05 | |
| 2,5-BTPEMTPS | 552 (–, –) green–yellow | 5.2 | 12560 | 1.98 | 6.40 | 2.45 | |
| 2,5-BTPEMTPS | ITO/NPB/BTPE: 2,5-BTPEMTPS ($x$ wt%)/TPBI/LiF/Al | | | | | | |
| $x = 10$ | 540 (–, –) green–yellow | 4.8 | 8894 | 2.13 | 6.64 | 3.36 | |
| $x = 20$ | 540 (–, –) green–yellow | 4.6 | 10480 | 2.18 | 7.02 | 3.24 | |
| $(VP)_3$-$(TPE)_3$ | ITO/NPB/$(VP)_3$-$(TPE)_3$/$Alq_3$/LiF/Al | | | | | | 58 |
| | 474 (0.18, 0.31) green–blue | 6.0 | 1908 | – | – | – | |

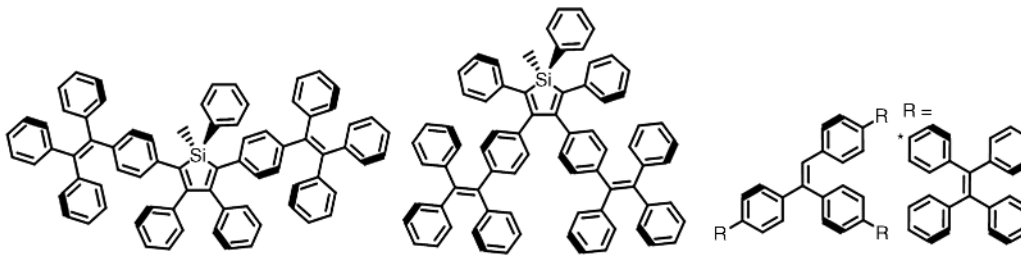


structural design herein. More TPE or triphenylethene AIE or AIEE materials containing an arylamine moiety are known in the literature. Arylamine-containing $C_4$ [60], TPATPE [61], 2TPATPE [61], TPE-2Cz [62], TPECa [63], and TPECaP [63] are all such materials. Their OLED data are all summarized in Table 1.12. Except for TPE-2Cz, most of the OLEDs show green–blue to blue–green EL with wavelengths in the range 484–514 nm. The TPE-2Cz OLED has an EL wavelength at 462 nm corresponding to 1931 $CIE_{x,y}$ (0.17, 0.21), approximately blue, but its EL efficiency is only moderate ($\eta_C = 2.80\,cd\,A^{-1}$, $\eta_P = 2.51\,lm\,W^{-1}$).

Fluorene (or the more rigid and bulky 9,9′-spirobifluorene) is the repeating unit of high-performance blue light-emitting polymers, polyfluorenes (PFs). The hybrid or fused structure of TPE and fluorene (or 9,9′-spirobifluorene) can take good advantage of the AIE or AIEE effect and high PL efficiency of blue emission. Three sets of such materials, BTPEBCF [64], SFTPE [62], and F$n$-TPE ($n = 1$–5) [65], are known in the literature (Table 1.13). Whereas SFTPE, F1-TPE, and F2-TPE OLEDs exhibit EL with wavelengths shorter than 470 nm, an empirical benchmark of blue color, BTPEBCF, F3-TPE, F4-TPE, and F5-TPE OLEDs all exhibit EL at wavelengths 476–508 nm, indicative of green–blue color. Regardless of the unsatisfactory blue color purity, the EL efficiency of BTPEBCF is the best; $\eta_C$ and $\eta_P$ can reach 7.9 cd $A^{-1}$ and 3.7 lm $W^{-1}$, respectively.

Organoboron compounds are particularly attractive and promising owing to their unique properties stemming from the $p_\pi$–$\pi^*$ conjugation between the vacant p orbital on the boron atom and the $p^*$ orbital of the $\pi$-conjugated framework. Organoboron compounds also have electron-transporting properties [66, 67]. A very high blue EL efficiency ($\eta_{EXT} > 6\%$) has been reported for D–$\pi$–A-type blue fluorophores containing dimesitylboron as electron acceptor [68]. In the literature, two TPE-containing organoboron compounds

***Table 1.12*** *Summary of reported OLEDs containing arylamine-based TPE derivative AIE or AIEE materials.*

| AIE or AIEE fluorophore | $\lambda_{max}^{EL}$, $CIE_{x,y}$, color code (nm), ($x$, $y$), color | $V_{on}$ (V) | $L_{max}$ (cd m$^{-2}$) | $\eta_{EXT}$ (%) | $\eta_C$ (cd A$^{-1}$) | $\eta_P$ (lm W$^{-1}$) | Ref. |
|---|---|---|---|---|---|---|---|
| $C_4$ | ITO/NPB/$C_4$/$Alq_3$/LiF/Al | | | | | | 60 |
| | 474 (–, –) green–blue | 6.0 | 548 | – | 2 | – | |
| EML | ITO/NPB/EML/TPBI/$Alq_3$/LiF/Al | | | | | | 61 |
| TPATPE | 492 (–, –) green–blue | 3.6 | 15480 | 3.4 | 8.6 | 5.3 | |
| 2TPATPE | 514 (–, –) blue–green | 3.4 | 32230 | 4.0 | 12.3 | 10.1 | |
| EML | ITO/EML/TPBI/$Alq_3$/LiF/Al | | | | | | |
| TPATPE | 492 (–, –) green–blue | 4.2 | 26090 | 3.3 | 8.3 | 4.9 | |
| 2TPATPE | 513 (–, –) blue–green | 3.2 | 33770 | 4.4 | 13.0 | 11.0 | |
| TPE-2Cz | ITO/NPB/TPE-2Cz/TPBI/LiF/Al | | | | | | 62 |
| | 462 (0.17, 0.21) blue | 3.3 | 6179 | – | 2.80 | 2.51 | |
| EML | ITO/NPB/EML/TPBi/$Alq_3$/LiF/Al | | | | | | 63 |
| TPECa | 484 (–, –) green–blue | 4.0 | 7508 | 1.8 | 3.8 | 2.7 | |
| TPECaP | 488 (–, –) green–blue | 3.8 | 11060 | 1.7 | 3.5 | 2.9 | |
| TTPECaP | 488 (–-, –-) green–blue | 4.0 | 13650 | 1.8 | 3.8 | 2.1 | |
| EML | ITO/EML/TPBI/LiF/Al | | | | | | |
| TPECaP | 496 (–, –) green–blue | 4.4 | 12930 | 2.2 | 5.5 | 3.8 | |
| TTPECaP | 490 (–, –) green–blue | 3.6 | 9048 | 2.3 | 6.3 | 4.1 | |

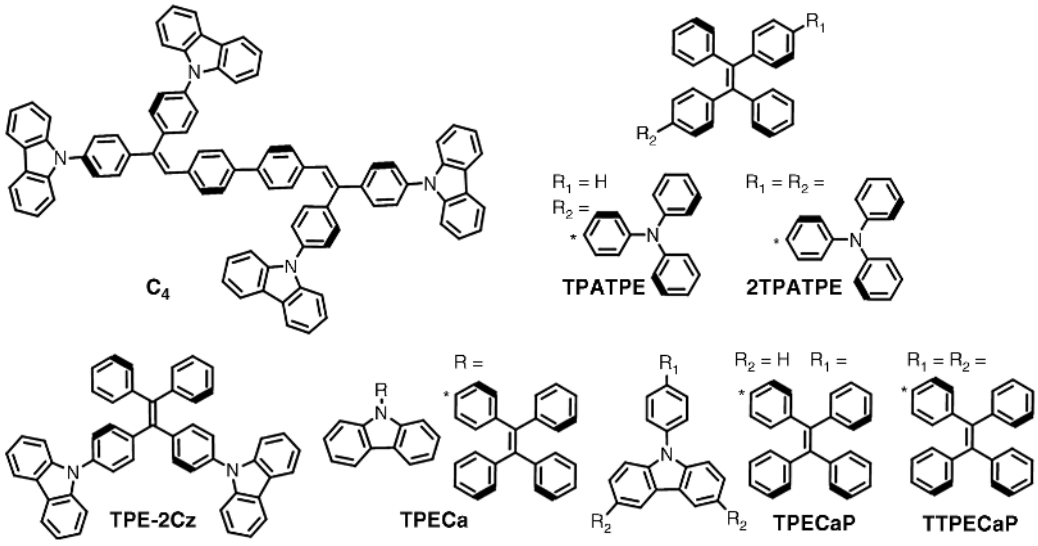


have been reported for OLED applications, TPEMesB and BTPEPBN (Table 1.14) [69, 70]. For TPEMesB OLEDs, it has been shown that the EL efficiency is in fact higher without using an ETL (TPBI) in the device, demonstrating the electron-transporting property in addition to the green–blue light-emitting function of TPEMesB AIE or AIEE materials. For BTPEPBN OLED, no EL wavelength was reported, but 'sky blue' color was mentioned for its PL, probably in the solid state. A BTPEPBN OLED was reported with low EL efficiency ($\eta_{EXT} = 1.52\%$, $\eta_C = 4.43\,cd\,A^{-1}$, $\eta_P = 1.64\,lm\,W^{-1}$), although it is better than the OLED

***Table 1.13*** *Summary of reported OLEDs containing fluorene- or 9,9′-spirobifluorene-based TPE derivative AIE or AIEE materials.*

| AIE or AIEE fluorophore | $\lambda_{max}^{EL}$, $CIE_{x,y}$, color code (nm), (*x*, *y*), color | $V_{on}$ (V) | $L_{max}$ (cd $m^{-2}$) | $\eta_{EXT}$ (%) | $\eta_C$ (cd $A^{-1}$) | $\eta_P$ (lm $W^{-1}$) | Ref. |
|---|---|---|---|---|---|---|---|
| BTPEBCF | ITO/NPB/BTPEBCF/TPBI/LiF/Al | | | | | | 64 |
| | 508 (0.24, 0.42) blue–green | 5.5 | 13760 | 2.6 | 7.2 | 2.8 | |
| | ITO/NPB/BTPEBCF/TPBI/$Alq_3$/LiF/Al | | | | | | |
| | 502 (0.21, 0.37) blue–green | 4.5 | 6400 | 2.9 | 7.9 | 3.7 | |
| SFTPE | ITO/NPB/SFTPE/TPBI/LiF/Al | | | | | | 62 |
| | 466 (0.18, 0.24) blue | 2.6 | 8196 | – | 3.33 | 2.10 | |
| EML | ITO/PEDOT/EML/TPBI/LiF/Al | | | | | | 65 |
| F1-TPE | 468 (–, –) blue | 5.8 | 1300 | – | 2.6 | 1.0 | |
| F2-TPE | 468 (–, –) blue | 5.5 | 1100 | – | 1.5 | 0.55 | |
| F3-TPE | 488 (–, –) green–blue | 6.4 | 1050 | – | 1.6 | 0.5 | |
| F4-TPE | 476 (–, –) green–blue | 6.2 | 1050 | – | 1.8 | 0.6 | |
| F5-TPE | 480 (–, –) green–blue | 4.8 | 120 | – | 0.2 | 0.06 | |

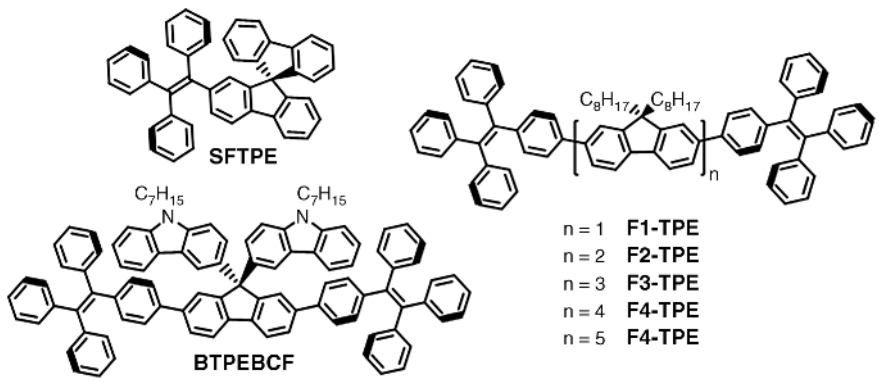


with the same organoboron material lacking two TPE substituents [70]. This is yet further experimental evidence supporting the AIE or AIEE effect of a TPE moiety that is beneficial for EL efficiency. Regarding electron transport of OLED materials, the other well-known electron transporting material is 2,5-diphenyl-1,3,4-oxadiazole structural moiety, and it has been attached with two TPE units to form OXa-*p*TPE and OXa-*m*TPE (Table 1.14) [71]. Although the AIE or AIEE effect has been demonstrated for both OXa-*p*TPE and OXa-*m*TPE compounds, high EL efficiency ($\eta_{EXT} = 5.0\%$, $\eta_C = 9.79$ cd $A^{-1}$, $\eta_P = 9.92$ lm $W^{-1}$) has been achieved with the dopant OLEDs, of which OXa-*p*TPE or OXa-*m*TPE are used as the host material for BUBD-1 blue dopant. Compared with the EL spectra of BUBD-1 reported elsewhere [72], the EL spectra shown in the paper on OXa-*p*TPE and OXa-*m*TPE OLEDs [71] indicate that it is a co-emission EL from both host and dopant and it is green–blue in color, 1931 $CIE_{x,y}$ (0.15, 0.34).

One large family of TPE derivatives is derived from attaching to or being attached with various polycyclic aromatic hydrocarbons (PAHs). TPTPE (or thiophene-based TPTDPE) and BTPTPE are the fused TPE dimer and trimer (Table 1.15), respectively, via one common benzene ring, the fundamental repeating unit of PAHs [73]. Whereas the trimer BTPTPE OLED exhibits very short wavelength EL at 448 nm, indicative of an authentic blue color, the TPTPE (or thiophene-based TPTDPE) OLED has a green–blue EL at

***Table 1.14*** *Summary of reported OLEDs containing organoboron- or 1,3,4-oxadiazole-based TPE derivative AIE or AIEE materials.*

| AIE or AIEE fluorophore | $\lambda_{max}^{EL}$, $CIE_{x,y}$, color code (nm), (*x*, *y*), color | $V_{on}$ (V) | $L_{max}$ (cd $m^{-2}$) | $\eta_{EXT}$ (%) | $\eta_C$ (cd $A^{-1}$) | $\eta_P$ (lm $W^{-1}$) | Ref. |
|---|---|---|---|---|---|---|---|
| TEPDMesB | ITO/NPB/TEPDMesB/LiF/Al | | | | | | 69 |
| | 496, 512 (–, –) green–blue | 6.3 | 5581 | 2.3 | 5.78 | 3.4 | |
| | ITO/NPB/TEPDMesB/TPBI/LiF/Al | | | | | | |
| | 496, 512 (–, –) green–blue | 6.3 | 5170 | 2.7 | 7.13 | 3.2 | |
| BTPEPBN | – | | | | | | 70 |
| | –, – (–, –) green–blue | – | – | 1.52 | 4.43 | 1.64 | |
| Oxa-*p*TPE | ITO/NPB/Oxa-*p*TPE:BUBD-1/TPBI/$Alq_3$/Al | | | | | | 71 |
| | ~500 (0.15, 0.34) green–blue | 5.1 | 10070 | 5.0 | 9.79 | 9.92 | |
| Oxa-*m*TPE | ITO/NPB/Oxa-*m*TPE:BUBD-1/TPBI/$Alq_3$/Al | | | | | | |
| | 500 (0.15, 0.33) green–blue | 6.25 | 7734 | – | 9.82 | 7.96 | |

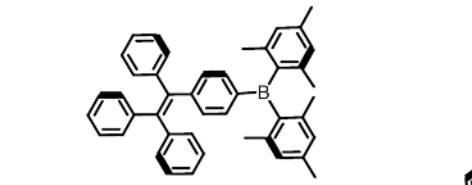


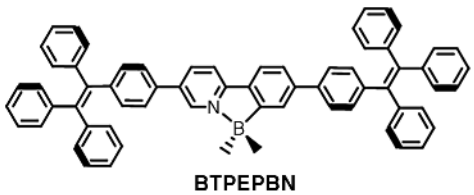


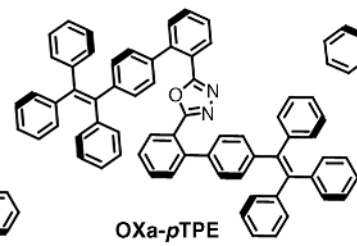


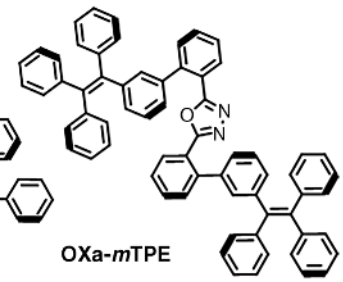


488 nm (512 nm for thiophene-based TPTDPE). The TPTPE OLED shows better EL efficiency than the other two. However, the green–blue EL efficiency of TPTPE is only fair ($\eta_{EXT} = 2.7\%$, $\eta_C = 5.8\,cd\,A^{-1}$, $\eta_P = 3.5\,lm\,W^{-1}$). PAHs such as pyrene, anthracene, phenanthrene, and naphthacene have been singly attached to TPE forming TPEPy, TPEAn, TPEPa, TPENp, and TPE-2-Np (Table 1.15) [74]. They are also doubly attached to TPE in forming TPEBPy, TPEBAn, TPEBPa, TPEBNp, and TPEB-2-Np (Table 1.15) [74]. Although the solid-state PL of TPENp has the shortest wavelength at 469 nm, TPEPa has the shortest EL wavelength at 464 nm, a possible blue color. The EL of TPENp is red shifted to 480 nm and becomes green–blue. A similar red shift, from the smallest +2 nm of TPEB-2-Np to the largest +30 nm of TEPBAn, are common for these two types of TPE derivatives, except one TPEPa, which has a blue-shifted rather than a red-shifted EL. All of the non-dopant OLEDs containing the materials mentioned here have EL efficiencies ranging from poor ($\eta_{EXT} = 1.3\%$, $\eta_C = 2.4\,cd\,A^{-1}$, $\eta_P = 1.1\,lm\,W^{-1}$ for TPENp OLED) to above average ($\eta_{EXT} = 3.0\%$, $\eta_C = 7.3\,cd\,A^{-1}$, $\eta_P = 5.6\,lm\,W^{-1}$ for TPEPy OLED). However, the performance of TPEPy OLED is not as good as that of another pyrene-containing TPE derivative OLED (TTPEPy) reported earlier, and both OLEDs have comparable green–blue color.

The latest member joining the family may be the mono-, di-, and triphenylethene *n*-hexyloxybenzene derivatives PhTPE, Ph2TPE, and Ph3TPE reported by Li and co-workers [75] (Table 1.15). It must be because of the steric hindrance twisting the coplanarity between the TPE unit and *ortho*-substituted *n*-hexyloxybenzene that the Ph2TPE OLED shows the shortest EL wavelength at 457 nm, an authentic blue

***Table 1.15*** *Summary of reported OLEDs containing PAH–TPE derivative AIE or AIEE materials.*

| AIE or AIEE fluorophore | $\lambda_{max}^{EL}$, $CIE_{x,y}$, color code (nm), ($x$, $y$), color | $V_{on}$ (V) | $L_{max}$ (cd $m^{-2}$) | $\eta_{EXT}$ (%) | $\eta_C$ (cd $A^{-1}$) | $\eta_P$ (lm $W^{-1}$) | Ref. |
|---|---|---|---|---|---|---|---|
| EML | ITO/NPB/EML/TPBI/LiF/Al | | | | | | 73 |
| BTPTPE | 448 (–, –) blue | 4.2 | 3530 | 1.6 | 2.8 | 1.4 | |
| TPTPE | 488 (–, –) green–blue | 4.2 | 10800 | 2.7 | 5.8 | 3.5 | |
| TPTDPE | 512 (–, –) blue–green | 4.2 | 7620 | 1.1 | 2.2 | 3.0 | |
| EML | ITO/NPB/EML/TPBI/$Alq_3$/LiF/Al | | | | | | 74 |
| TPEPy | 484 (–, –) green–blue | 3.6 | 13400 | 3.0 | 7.3 | 5.6 | |
| TPEAn | 486 (–, –) green–blue | 4.0 | 8410 | 2.1 | 4.6 | 3.7 | |
| TPEPa | 464 (–, –) blue | 5.2 | 4600 | 1.4 | 2.7 | 1.6 | |
| TPENp | 480 (–, –) green–blue | 6.0 | 4120 | 1.3 | 2.4 | 1.1 | |
| TPE-2-Np | 492 (–, –) green–blue | 3.8 | 19800 | 2.7 | 7.3 | 4.2 | |
| TPEBPy | 516 (–, –) blue–green | 4.8 | 13370 | 2.0 | 5.8 | 2.0 | |
| TEPBAn | 516 (–, –) blue–green | 6.0 | 22600 | 2.0 | 5.7 | 2.0 | |
| TPEBPa | 488 (–, –) green–blue | 4.8 | 9250 | 2.6 | 5.5 | 3.5 | |
| TPEBNp | 488 (–, –) green–blue | 5.4 | 7130 | 1.9 | 4.2 | 2.3 | |
| TPEB-2-Np | 494 (–, –) green–blue | 4.4 | 13500 | 2.5 | 6.1 | 3.7 | |
| EML | ITO/NPB/EML/TPBI/LiF/Al | | | | | | |
| TPEBPy | 516 (–, –) blue–green | 4.6 | 25500 | 2.1 | 6.1 | 2.7 | |
| TEPBAn | 512 (–, –) blue–green | 4.4 | 14750 | 1.9 | 5.1 | 3.0 | |
| EML | ITO/$MoO_3$/NPB/EML/TPBI/LiF/Al | | | | | | 75 |
| PhTPE | 488 (0.19, 0.30) green–blue | 4.1 | 3966 | – | 5.0 | 3.87 | |
| Ph2TPE | 457 (0.16, 0.15) blue | 4.1 | 1261 | – | 2.3 | 1.70 | |
| Ph3TPE | 467 (0.17, 0.20) blue | 3.7 | 2497 | – | 3.7 | 2.50 | |

BTPTPE

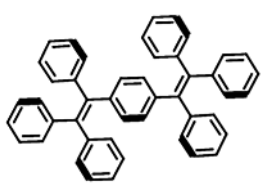

TPTPE

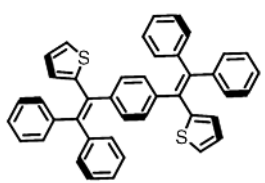


TPTDPE

(*continued*)

***Table 1.15*** (*Continued*)

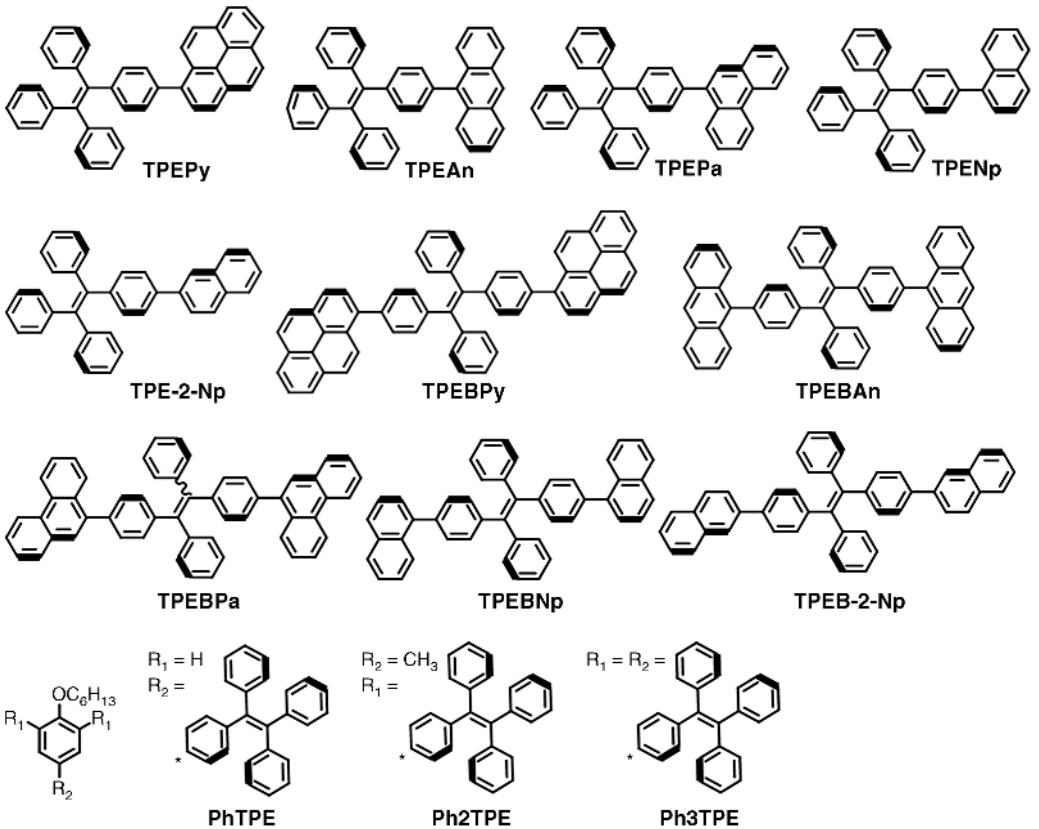

corresponding to 1931 $CIE_{x,y}$ (0.16, 0.15). Similarly to several of the TPE derivatives shown earlier, Ph2TPE OLED has an unusually blue-shifted EL compared with its solid-state PL at 494–498 nm. Nevertheless, the EL efficiency of the Ph2TPE OLED is not good ($\eta_C = 2.3\,cd\,A^{-1}$, $\eta_P = 1.7\,lm\,W^{-1}$) and that of Ph3TPE OLED [also with a blue EL at 467 nm and 1931 $CIE_{x,y}$ (0.17, 0.20)] is better ($\eta_C = 3.7\,cd\,A^{-1}$, $\eta_P = 2.5\,lm\,W^{-1}$).

As we have seen with the many triphenylethene or TPE derivatives so far, they mostly exhibit EL with green–blue, blue–green, green, and even yellow–green color, and these are not the desirable colors in display applications. From this survey, it is evident that authentic blue AIE or AIEE materials containing a triphenylethene or TPE moiety are difficult to come by. The last group in the family of triphenylethene or TPE derivatives are the AIE or AIEE effects shown in the other extreme of visible spectra, namely the long wavelengths in the orange, red, and even near-IR region. In order to acquire a long emission wavelength, either PL or EL, the triphenylethene or TPE moiety has to be π-conjugated to a strong electron acceptor. From a survey of the literature, it was found that the benzo[*c*][1,2,5]thiadiazole (BTZ) moiety seems to be the most potent electron acceptor for long-wavelength PL or EL (Table 1.16).

For EL wavelengths longer than 650 nm, a benchmark for red color, thiophene-bridged triphenylethene and BTZ is necessary and it requires two thiophene bridges (like BTPEBTTD) instead of one thiophene (like BTPETTD) or two benzene bridges (BTPETD) (Table 1.16) [78]. This is because the thiophene ring has a lower bandgap energy than the benzene ring. Similarly, for $V_2BV_2$ and $T_2BT_2$ (Table 1.16) [79], a C=C double bond as the connecting π-conjugation bridge is not good enough to extend the EL wavelength beyond 650 nm, even though there is a strong electron donor triphenylamine between the triphenylethene and BTZ. Another approach is to increase the electron-deficient power of BTZ by changing to [1,2,5]thiadiazolo[3,4-*g*]quinoxaline (QTD) of TPEQTD or MTPEQTD, or benzo[1,2-*c*;4,5-*c*′]bis[1,2,5]thiadiazole (BBTD) of TPEBBTD or MTPEBBTD (Table 1.16). [80] These four compounds (TPEQTD, MTPEQTD, TPEBBTD, and MTPEBBTD) have EL wavelengths in the range 706–864 nm, within the near-IR region. However, their EL $L_{max}$ are all low and none of their $\eta_{EXT}$ values is over 1%. The most successful design for red EL is the branched version of BTPEBTTD, that is, TBTPEBTTD (Table 1.16) [28]. TBTPEBTTD has an EL wavelength at 650 nm, 1931 $CIE_{x,y}$ (0.67, 0.32), at the edge of red color on the chromaticity diagram. It was reported with $\eta_{EXT}$ as high as 3.7%, superior to the 3.1% of the FPhSPFN OLED [27], one of the most efficient nondopant red OLEDs based on AIE or AIEE materials.

## 1.8 White OLEDs Containing AIE or AIEE Materials

Although its AIE or AIEE effect was demonstrated above, the blue fluorophore DPVBi was utilized in RGB multi-color OLED displays as early as 1997 [81]. For white EL used for lighting, there are a number of materials and device configurations for generating white EL from a DPVBi-containing OLED (Table 1.17) [38, 82–86]. In terms of EL efficiency and $L_{max}$, a DPVBi blue-emitting layer doped with yellow–orange rubrene is probably the best approach, as reported by Li and Shinar [83] Such a WOLED exhibits EL with 1931 $CIE_{x,y}$ (0.27, 0.31) near-white chromaticity, $L_{max}$ as high as $50100\,cd\,m^{-2}$, $\eta_{EXT}$ 4.0% and $\eta_P$ 3.9 lm $W^{-1}$. However, since it is a two-color-white WOLED, it is not possible for the CRI to be high (the original paper did not report the CRI value of the device).

The second kind of AIE or AIEE material being used in WOLEDs is the orange–red fluorophore NPAFN (Table 1.3 and Table 1.17) [87]. Taking advantage of its strong AIE or AIEE effect reported by Chen and coworkers, NPAFN enabled the first all-nondopant three-color WOLED to be obtained. Because of its nondopant nature, the NPAFN WOLED showed almost constant white chromaticity with 1931 $CIE_{x,y}$ (0.34, 0.38) and a good CRI of ∼80, although its EL efficiency was only fair ($\eta_{EXT} = 3.4\%$, $\eta_P = 9.1\,cd\,A^{-1}$ at $1000\,cd\,m^{-2}$).

***Table 1.16*** *Long-wavelength EL from OLEDs with TPE-containing AIE or AIEE materials.*

| AIE or AIEE fluorophore | $\lambda_{max}^{EL}$, $CIE_{x,y}$, color code (nm), (*x*, *y*), color | $V_{on}$ (V) | $L_{max}$ (cd $m^{-2}$) | $\eta_{EXT}$ (%) | $\eta_C$ (cd $A^{-1}$) | $\eta_P$ (lm $W^{-1}$) | Ref. |
|---|---|---|---|---|---|---|---|
| BTPETTD | ITO/NPB/BTPETTD/TPBI/$Alq_3$/LiF/Al | | | | | | 76 |
| | 592 (0.61, 0.39) orange | – | 11000 | – | 4.2 | 2.7 | |
| BTPETTD | ITO/BTPETTD/TPBI/LiF/Al | | | | | | 77 |
| | 592 (–, –) orange | <6 | ~400 | | 7.0[a] | 3.2[a] | |
| | ITO/NPB/BTPETTD/TPBI/LiF/Al | | | | | | |
| | 592 (–, –) orange | <5 | ~20000 | | 3.5[a] | 1.7[a] | |
| EML | ITO/NPB/EML/TPBI/$Alq_3$/LiF/Al | | | | | | 78 |
| BTPETTD | 540 (–, –) green–yellow | 3.9 | 13540 | 1.5 | 5.2 | 3.0 | |
| BTPETD | 592 (–, –) orange | 5.4 | 8330 | 3.1 | 6.4 | 2.9 | |
| BTPEBTTD | 668 (–, –) red | 4.4 | 1640 | 1.0 | 0.4 | 0.5 | |
| EML | ITO/NPB/EML/TPBI/LiF/Al | | | | | | 79 |
| $V_2BV_2$ | 616 (–, –) red–orange | 3.3 | 10573 | 2.53 | 4.24 | 4.06 | |
| $T_2BT_2$ | 590 (–, –) orange | 4.3 | 13535 | 2.88 | 6.81 | 4.96 | |
| EML | ITO/$MoO_3$/NPB/EML/TPBI/$Alq_3$/LiF/Al | | | | | | 80 |
| TPEQDT | 706 (–, –) near-IR | 5.5 | 2917[b] | 0.89 | – | – | |
| MTPEQDT | 749 (–, –) near-IR | 4.6 | 1576[b] | 0.29 | – | – | |
| TPEBBTD | 802 (–, –) near-IR | 4.5 | 1604[b] | 0.43 | – | – | |
| MTPEBBTD | 864 (–, –) near-IR | 4.4 | 1003[b] | 0.20 | | | |
| TTPEBTTD | ITO/NPB/TTPEBTTD/TPBI/LiF/Al | | | | | | 28 |
| | 650 (0.67, 0.32) red | 4.2 | ~3000 | 3.7 | 2.4 | – | |

[a] At 1000 cd $m^{-2}$.
[b] In units of mW $Sr^{-1}$ $m^{-2}$.

***Table 1.16*** (*Continued*)

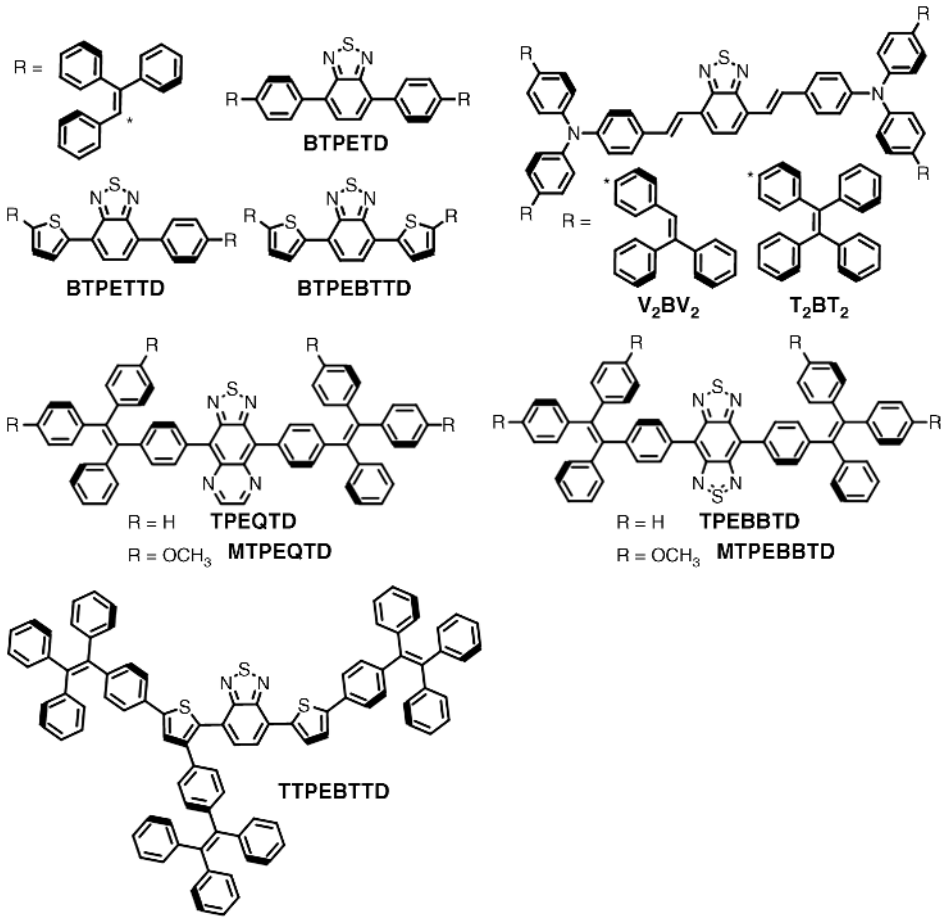

***Table 1.17*** *Summary of reported WOLEDs containing AIE or AIEE materials.*

| Fluorophore | $\lambda_{max}^{EL}$, $CIE_{x,y}$, CRI (nm), (*x*, *y*), CRI | $V_{on}$ (V) | $L_{max}$ (cd m$^{-2}$) | $\eta_{EXT}$ (%)[a] | $\eta_C$ (cd A$^{-1}$)[a] | $\eta_P$ (lm W$^{-1}$)[a] | Ref. |
|---|---|---|---|---|---|---|---|
| DPVBi | ITO/NPB:DCM2/DPVBi/$Alq_3$/CsF/Al | | | | | | 38 |
| | 445 (456), 570 (0.40, 0.37), – | – | 5400 | 3.0 | – | 2.4 | |
| | ITO/CuPc/NPB/DPVBi:DCM2/$Alq_3$:C-6/$Alq_3$/LiF/Al | | | | | | 82 |
| | 456, 515, 560 (0.30,0.36), – | 2.5 | >9000 | – | – | 5[b] | |
| | ITO/CuPc/NPB/DPVBi:rubrene/$Alq_3$/CsF/Al | | | | | | 83 |
| | 456, 560 (0.27, 0.31), – | <5 | 50100 | 4.0 | – | 3.9 | |
| | ITO/NPB/rubrene/DPVBi/$Alq_3$/LiF/Al | | | | | | 84 |
| | 456, 560 (0.30, 0.32), – | <3 | 17000 | – | 5.8 | 2.5 | |
| | ITO/NPB/DCM1/DPVBi/$Alq_3$/LiF/Al | | | | | | 85 |
| | 456, 564 (0.31, 0.33), – | ~3 | 3750 | – | – | 1.1 | |
| | ITO/NPB/DPVBI/$Alq_3$/LiF/Al | | | | | | 86 |
| | 456, 490, 520, 560, 600 (0.24, 0.30), – | – | 2330 | – | – | <1 | |
| NPAFN | ITO/NPB/NPAFN/Alq3/BCP/TPAOXD/TPBI/LiF/Al | | | | | | 87 |
| | 460, 520, 615 (0.34, 0.38), ~80 | – | 25000 | 2.9 | – | 2.1 | |
| TPVAn | ITO/PEDOT/NPB/TPVAn:DCJTB/TPBI/Mg:Ag/Ag | | | | | | 44 |
| | 456, 556 (0.33, 0.39), – | 9.3 | 30000 | 3.4[c] | 9.1[c] | – | |
| BTPETTD | ITO/NPB/BTPETTD/TTPEPy/TPBI/$Alq_3$/LiF/Al | | | | | | 76 |
| TTPEPy | 472, 492, 524 (0.42, 0.39), 85 | – | 15000 | – | ~6 | – | |
| | ITO/NPB/BTPETTD/NPB/TTPEPy/TPBI/$Alq_3$/LiF/Al | | | | | | |
| | 472, 492, 524 (0.40, 0.42), 90 | – | 18000 | – | ~7 | – | |
| TDPVBi | ITO/NPB//TDPVBi/CN-DPASDB/TPBI/LiF/Al | | | | | | 30 |
| CN-DPASDB | 468, 579 (0.24–0.36, 0.29–0.38), – | 3.5 | 25350 | – | ~4.5 | – | |
| | ITO/NPB/CN-DPASDB/NPB/TDPVBi/TPBI/LiF/Al | | | | | | |
| | 468, 579 (0.28, 0.34), – | 4.0 | 19450 | – | 7.1 | – | |
| BTPETTD | ITO/BTPETTD/DPPI/LiF/Al | | | | | | 77 |
| DPPI | 465, 592 (0.31, 0.31), 92 | 7.6 | >11000 | | 4.2 | 1.1 | |
| BTPETTD | ITO/$MoO_3$/TCTA/CDBP:FIrpic/TAZ/BPhen/Ag/Yb/BTPETTD(*x* nm) | | | | | | 88 |
| FIrpic | | | | | | | |
| $x = 190$ | 472, 550, 610 (>0.34, >0.35), – | – | ~30000 | ~6.8 | ~18.3 | ~7.2 | |
| $x = 240$ | 472, 610 (0.34, 0.35), – | – | ~6000 | ~5.8 | ~17.1 | ~6.6 | |
| OTB | ITO/NPB/OTB/T4AC/TPBI/LiF/Al | | | | | | 89 |
| T4AC | 436, 552 (0.31–0.34, 0.32–0.38), – | 2.8 | – | – | ~1.0 | – | |
| | ITO/NPB/OTB/T4AC/OTB/TPBI/LiF/Al | | | | | | |
| | 436, 552 (0.33–0.36, 0.35–0.38), – | 3.1 | – | – | ~0.9 | – | |

[a] At 1000 cd m$^{-2}$.
[b] At 10 cd m$^{-2}$.
[c] At 100 mA cm$^{-2}$ and >2000 cd m$^{-2}$.

**Table 1.17** (*Continued*)

The next WOLED containing AIE or AIEE materials to be reported was the efficient blue fluorophore TPVAn (Table 1.5 and 1.17) [44]. It adopted a two-color-white approach including the commercially available red dopant DCJTB. Although it has good white chromaticity [1931 $CIE_{x,y}$ (0.33, 0.39)], $L_{max}$ ($\sim$30 000 cd m$^{-2}$), and EL efficiency ($\eta_{EXT} = 3.4\%$, $\eta_C = 9.1$ lm W$^{-1}$ at 100 mA cm$^{-2}$ and >2000 cd m$^{-1}$), its CRI cannot be high, which was not mentioned in the reported paper.

Two other WOLEDs are based on all-AIE or -AIEE materials as the nondopant light-emitting layers appear. As shown in Table 1.17, Ma and co-workers reported all-AIE or -AIEE material-containing WOLEDs with blue TDPVBi (Table 1.6) and yellow CN-DPASDB (Table 1.3) [30]. At almost at the same time, Tang and co-workers reported WOLEDs with green–blue TTPEPy (Table 1.9) and orange BTPETTD (Table 1.16) [76]. Under lighting condition 1000 cd m$^{-2}$, the best $\eta_C$ of both sets of the WOLEDs can reach 7 cd A$^{-1}$, which is the highest among all fluorescence-based WOLEDs in Table 1.17. The white color chromaticity of TTPEPy/BTPETTD WOLED is 1931 $CIE_{x,y}$ (0.42, 0.39) or (0.40, 0.42), which is somewhat off from standard white 1931 $CIE_{x,y}$ (0.33, 0.33). Surprisingly, these TTPEPy/BTPETTD WOLEDs exhibit very high CRI, 85 or 90, which is extremely rare for two-color-white WOLEDs. According to the paper on the TTPEPy/BTPETTD WOLED [76], the multiple-emission peaks centered at 524, 492, and 472 nm were attributed to TTPEPy (492 nm) and impurities (524 and 472 nm), resulting in a broad EL band and hence unusually high CRI. In terms of EL efficiency, TDPVBi/CN-DPASDB WOLEDs are comparable to TTPEPy/BTPETTD WOLEDs, although the former are superior in white color chromaticity.

The orange BTPETTD AIE or AIEE material has been used in two other sets of WOLEDs. First, it was assembled with a non-AIE or -AIEE blue emitter, 4,4′-bis(1-phenyl-1*H*-phenanthro[9,10-*d*]imidazol-2-yl) biphenyl (DPPi) into a bilayer WOLED (Table 1.17) [77]. Owing to the uncommon energy level alignment between BTPETTD and DPPi, the blue emission is due to direct recombination of excitons in DPPi, whereas the red emission originates not only from the direct recombination of excitons in BTPETTD but also from a color down-conversion process by absorbing blue emission and re-emitting red photons. The combination of blue emission and red emission yields an efficient and extremely stable white color, regardless of the driving voltages. Once again, multiple-emission bands were observed for such WOLEDs and an unusually high CRI of 92 was achieved with excellent white color chromaticity, 1931 $CIE_{x,y}$ (0.31, 0.31). Second, BTPETTD has been used as a color down-conversion (CCL) capping layer of a top-emitting blue phosphorescence OLED (having FIrpic as the green–blue phosphorescence dopant) in generating good-quality white EL, 1931 $CIE_{x,y}$ (0.34, 0.35) (Table 1.17) [88]. At 914 cd m$^{-2}$, a common lighting condition, the phosphorescence–fluorescence hybrid white EL efficiency ($\eta_C = 17$–$18$ cd A$^{-1}$, $\eta_P = 6$–$7$ lm W$^{-1}$) is better than that of most fluorescence-based WOLEDs.

The last pair of compounds for WOLEDs is OTB (blue emission at 433 nm) and T4AC (yellow emission at 551 nm), reported by Gao and co-workers [89] (Table 1.17). Compared with those commonly seen with AIE or AIEE effects, the chemical structures of OTB and T4AC are unconventional and previously unknown. Yellow T4AC was reported with a large Stokes shift of 182 nm without self-absorption in the solid state, which is attributed to the excited-state intramolecular proton transfer property, providing the potential for solid-state emitters. Nevertheless, although good quality and stability of the white EL were reported (Table 1.17), the EL efficiency of the WOLED was rather poor under lighting conditions ($\eta_C \approx 1$ cd A$^{-1}$).

## 1.9 Perspectives

As shown in this chapter, it has been demonstrated repeatedly that the AIE or AIEE effect is effective in promoting the EL efficiency of nondopant OLEDs. Without AIE or AIEE materials, nondopant OLEDs, which are simple and easy to fabricate, show insufficient EL efficiency for practical application. In terms of

EL color purity, it is more successful for red than blue color; although there are many more AIE or AIEE materials available for green–blue or blue–green EL color, authentic blue EL of AIE or AIEE materials is still rare and needs further research and development. Although EL polymers derived from AIE or AIEE small-molecule materials have been reported in the literature, the AIE or AIEE effect of a small molecule does not necessarily remain in the polymeric form [90, 91]. They are not included in this chapter mainly because their OLED performances are far from satisfactory. Polymeric AIE or AIEE materials have potential for OLED applications but their device performances need improvement or a better design is needed for polymeric AIE or AIEE materials. Similarly, all or partial AIE or AIEE material-based WOLEDs are difficult to come by and not many of them have been reported. For practical lighting conditions, none of them is good enough in terms of EL efficiency. For lighting application of OLEDs, phosphorescence-based materials have a better chance of success, and this is one potential material that may be suitable for demonstrating the AIE or AIEE effect, although so far there are no literature reports.

## References


1. Tang, C.W., and VanSlyke, S.A. (1987) Organic electroluminescent diodes. *Appl. Phys. Lett.*, **51**, 913–915.
2. Chen, C.-T. (2004) Evolution of red organic light-emitting diodes: materials and devices. *Chem. Mater.*, **16**, 4389–4400.
3. Shih, P.-I., Chien, C.-H., Wu, F.-I., and Shu, C.-F. (2007) A novel fluorene–triphenylamine hybrid that is a highly efficient host material for blue-, green-, and red-light-emitting electrophosphorescent devices. *Adv. Funct. Mater.*, **17**, 3514–3520.
4. Tsutsui, T. (1997) Progress in electroluminescent devices using molecular thin films. *MRS Bull.*, **22**(6), 39–45.
5. Su, S.-J., Sasabe, H., Tekeda, T., and Kido, J. (2008) Pyridine-containing bipolar host materials for highly efficiency blue phosphorescent OLEDs. *Chem. Mater.*, **20**, 1691–1693.
6. Su, S.-J., Gonmori, E., Sasabe, H., and Kido, J. (2008) Highly efficient organic blue- and white-light-emitting devices having a carrier- and exciton-containing structure for reduced efficiency roll-off. *Adv. Mater.*, **20**, 4189–4194.
7. Kim, D.H., Cho, N.S., Oh, H.-Y., Yang, J.H., Jeon, W.S., Park, J.S., Suh, M.C., and Kwon, J.H. (2011) Highly efficient red phosphorescent dopants in organic light-emitting devices. *Adv. Mater.*, **23**, 2721–2726.
8. Chen, H.Y., Lam, W.Y., Luo, J.D., Ho, Y.L., Tang, B.Z., Zhu, D.B., Wong, M., and Kwok, H.S. (2002) Highly efficient organic light-emitting diodes with a silole-based compound. *Appl. Phys. Lett.*, **81**, 574–576.
9. McKittrick, J. (2002) *Luminescent Inorganic Materials*, http://www.4physics.com/phy_demo/glow/luminescent.html (last accessed 7 May 2013).
10. Tang, B.Z., Zhan, X., Yu, G., Lee, P.P.S., Liu, Y., and Zhu, D. (2001) Efficient blue emission from siloles. *J. Mater. Chem.*, **11**, 2974–2978.
11. Luo, J., Xie, Z., Lam, J.W.Y., Cheng, L., Chen, H., Qiu, C., Kwok, H.S., Zhan, X., Liu, Y., Zhu, D., and Tang, B.Z. (2001) Aggregation-induced emission of 1-methyl-1,2,3,4,5-pentaphenylsilole. *Chem. Commun.* 1740–1741.
12. Murata, H., Kafafi, Z.H., and Uchida, M. (2002) Efficient organic light-emitting diodes with undoped active layers based on silole derivatives. *Appl. Phys. Lett.*, **80**, 189–191.
13. Murata, H., Malliaras, G.G., Uchida, M., Shen, Y., and Kafafi, Z.H. (2001) Non-dispersive and air-stable electron transport in an amorphous organic semiconductor. *Chem. Phys. Lett.*, **339**, 161–166.
14. Palilis, L.C., Murata, H., Uchida, M., and Kafafi, Z.H. (2003) High efficiency molecular organic light-emitting diodes based on silole derivatives and their exciplexes. *Org. Electron.*, **4**, 113–121.
15. Chen, J., Law, C.C.W., Lam, J.W.Y., Dong, Y., Lo, S.M.F., Williams, I.D., Zhu, D., and Tang, B.Z. (2003) Synthesis, light emission, nanoaggregation, and restricted intramolecular rotation of 1,1-substituted 2,3,4,5-tetraphenylsiloles. *Chem. Mater.*, **15**, 1535–1546.
16. Li, Z., Dong, Y., Mi, B., Tang, Y., Häussler, M., Tong, H., Dong, Y., Lam, J.W.Y., Ren, Y., Sung, H.H.Y., Wong, K. S., Gao, P., Williams, I.D., Kwok, H.S., and Tang, B.Z. (2005) Structural control of the photoluminescence of silole regioiomers and their utility as sensitive regiodiscriminating chemosensors and efficient electroluminescent materials. *J. Phys. Chem. B*, **109**, 10061–10066.

17. Lee, J., Yuan, Y.-Y., Kang, Y., Jia, W.-L., Lu, Z.-H., and Wang, S. (2006) 2,5-Functionalized spiro-bisiloles as highly efficient yellow-light emitters in electroluminescent devices. *Adv. Funct. Mater.*, **16**, 681–686.
18. Mei, J., Wang, J., Sun, J.Z., Zhao, H., Yuan, W., Deng, C., Chen, S., Sung, H.H.Y., Lu P., Qin, A., Kwok, H.S., Ma, Y., Williams, I.D., and Tang, B.Z. (2012) Siloles symmetrically substituted on their 2,5-positions with electron-accepting and donating moieties: facile synthesis, aggregation-enhanced emission, solvatochromism, and device application. *Chem. Sci.*, **3**, 549–558.
19. Jiang, T., Jiang, Y., Qin, W., Chen, S., Lu, Y., Lam, J.W.Y., He, B., Lu, P., Sung, H.H.Y., Williams, I.D., Kwok, H.S., Zhao, Z., Qiu, H., and Tang, B.Z. (2012) Naphthalene-substituted 2,3,4,5-tetraphenylsiloles: synthesis, structure, aggregation-induced emission and efficient electroluminescence. *J. Mater. Chem.*, **22**, 20266–20272.
20. Wu, W.-C., Yeh, H.-C., Chan, L.-H., and Chen, C.-T. (2002) Red organic light-emitting diode with a non-doping amorphous red emitter. *Adv. Mater.*, **14**, 1072–1075.
21. Yeh, H.-C., Chan, L.-H., Wu, W.-C., and Chen, C.-T., (2003) Non-doped red organic light-emitting diodes. *J. Mater. Chem.*, **14**, 1293–1298.
22. Yeh, T.-S., Chow, T.J., Tsai, S.-H., Chiu, C.-W., and Zhao, C.-X., (2006) Electroluminescence of bisindolylmaleimide derivatives containing pentafluorophenyl substituents. *Chem. Mater.*, **18**, 832–839.
23. Kuo, W.-J., Chen, Y.-H., Jeng, R.-J., Chan, L.-H., Lin, W.-P., and Yang, Z.-M. (2007) Peripheral aryl-substituted pyrrole fluorophores for glassy blue-light-emitting diodes. *Tetrahedron*, **63**, 7086–7096.
24. Lee, Y.-S., Lin, Z., Chen, Y.-Y., Liu, C.-Y., and Chow, T.J. (2010) Asymmetric indolylmaleimides as non-dopant type red color emitting dyes. *Org. Electron.*, **11**, 604–612.
25. Luo, F.-T., Tao, Y.-T., Ko, S.-L., Chuen, C.-H., and Chen, H. (2002) Efficient electroluminescent material for light-emitting diodes from 1,4-distryrylbenzene derivatives. *J. Mater. Chem.*, **12**, 47–52.
26. Yeh, H.-C., Yeh, S.-J., and Chen, C.-T. (2003) Readily synthesised arylamino fumaronitrile for non-doped red organic light-emitting diodes. *Chem. Commun.* 2632–2633.
27. Lee, Y.-T., Chiang, C.-L., and Chen, C.-T. (2008) Solid-state highly fluorescent diphenylaminospirobifluorenefumaronitrile red emitters for non-doped organic light-emitting diodes. *Chem. Commun.* 217–219.
28. Zhao, Z., Geng, J., Chang, Z., Chen, S., Deng, C., Jiang, T., Qin, W., Lam, J.W.Y., Kwok, H.S., Qiu, H., Liu, B., and Tang, B.Z. (2012) A tetraphenylethene-based red luminophor for an efficient non-doped electroluminescence device and cellular imaging. *J. Mater. Chem.*, **22**, 11018–11021.
29. Zhang, W., He, Z., Mu, L., Zou, Y., Wang, Y., and Zhao, S. (2010) Red non-doped electroluminescent dyes based on arylaminofumaronitrile derivatives. *Dyes Pigments*, **85**, 86–92.
30. Liu, S., Li, F., Diao, Q., and Ma, Y. (2010) Aggregation-induced enhanced emission materials for efficient white organic light-emitting devices. *Org. Electron.*, **11**, 613–617.
31. Wang, B., Wang, Y., Hua, J., Jiang, Y., Huang, J., Qian, S., and Tian, H. (2011) Starburst triarylamine donor–acceptor–donor quadrupolar derivatives based on cyano-substituted diphenylaminestyrylbenzene: tunable aggregation-induced emission colors and large two-photon absorption cross sections. *Chem. Eur.J.*, **17**, 2647–2655.
32. Ning, Z., Chen, Z., Zhang, Q., Yan, Y., Qian, S., Cao, Y., and Tian, H. (2007) Aggregation-induced emission (AIE)-active starburst triarylamine fluorophores as potential non-doped red emitters for organic light-emitting diodes and $Cl_2$ gas chemodosimeter. *Adv. Funct. Mater.*, **17**, 3799–3807.
33. Qian, G., Dai, B., Luo, M., Yu, D., Zhan, J., Zhang, Z., Ma, D., and Wang, Z.Y. (2008) Band gap tunable, donor–acceptor–donor charge-transfer heteroquinoid-based chromophores: near-infrared photoluminescence and electroluminescence. *Chem. Mater.*, **20**, 6208–6212.
34. Hosokawa, C., Higashi, H., Nakamura, H., and Kusumoto, T. (1995) Highly efficient blue electroluminescence from a distyrylarylene emitting layer with a new dopant. *Appl. Phys. Lett.*, **67**, 3853–3856.
35. Turro, N.J. (1991) *Modern Molecular Photochemistry*, University Science Books, Sausalito, CA, pp. 170–172.
36. Wang, S., Oldham, W.J., Jr, Hudack, R.A., Jr, and Bazan, G.C. (2000) Synthesis, morphology, and optical properties of tetrahedral oligo(phenylenevinylene) materials. *J. Am. Chem. Soc.*, **122**, 5695–5709.
37. Shaheen, S.E., Jabbour, G.E., Morrell, M.M., Kawabe, Y., Kippelen, B., Peyghambarian, N., Nabor, M.-F., Schlaf, R., Mash, E.A., and Armstrong, N.R. (1998) Bright blue organic light-emitting diode with improved color purity using a LiF/Al cathode. *J. Appl. Phys.*, **84**, 2324–2326.

38. Cheon, K.O., and Shinar, J. (2002) Bright white small molecular organic light-emitting devices based on a red-emitting guest-host layer and blue-emitting 4,4′-bis(2,2′-diphenylvinyl)-1,1′-biphenyl. *Appl. Phys. Lett.*, **81**, 1738–1741.
39. Xie, W., Hou, J., and Liu, S. (2003) Blue and white organic light-emitting diodes based on 4,4′-bis(2,2′-diphenylvinyl)-1,1′-biphenyl. *Semicond. Sci. Technol.*, **18**, L42–L44.
40. Ono, K., Hiei, T., and Saito, K. (2006) Synthesis and luminescent properties of bis(fluoren-9-ylidenemethyl)aromatics: green and red materials in organic electroluminescent devices. *Heterocycles*, **68**, 667–672.
41. Kim, S.-K., Park, Y.-I., Kang, I.-N., and Park, J.-W. (2007) New deep-blue emitting materials based on fully substituted ethylene derivatives. *J. Mater. Chem.*, **17**, 4670–4678.
42. Liu, S., He, F., Wang, H., Xu, H., Wang, C., Li, F., and Ma, Y. (2008) Cruciform DPVBi: synthesis, morphology, optical and electroluminescent properties. *J. Mater. Chem.*, **18**, 4802–4807.
43. Wen, S.-W., Lee, M.-T., and Chen, C.H. (2005) Recent development of blue fluorescent OLED materials and devices. *J. Displ. Technol.*, **1**, 90–99.
44. Shih, P.-I., Chung, C.-Y., Chien, C.-H., Diau, E.W.-G., and Shu, C.-F. (2007) Highly efficient non-doped blue-light-emitting diodes based on an anthrancene derivative end-capped with tetraphenylethylene groups. *Adv. Funct. Mater.*, **17**, 3141–3146.
45. Pope, M., Kallmann, H.P., and Magnante, P. (1963) Electroluminescence in organic crystals. *J. Chem. Phys.*, **38**, 2042–2043.
46. Krasovitskii, B.M., and Bolotin, B.N. (translated by Vopian, V. G.) (1988) *Organic Luminescent Materials*, VCH Verlag GmbH, Weinheim, p. 27.
47. Tong, H., Dong, Y., Hong, Y., Häussler, M., Lam, J.W.Y., Sung, H.H.Y., Yu, X., Sun, J., Williams, I.D., Kwok, H.S., and Tang, B.Z. (2007) Aggregation-induced emission: effects of molecular structure, solid-state conformation, and morphological packing arrangement on light-emitting behaviors of diphenyldibenzofulvene derivatives. *J. Phys. Chem. C*, **111**, 2287–2294.
48. Chen, H.Y., Lam, W.Y., Luo, J.D., Ho, Y.L., Tang, B.Z., Zhu, D.B., Wong, M., and Kwok, H.S. (2002) Highly efficient organic light-emitting diodes with a silole-based compound. *Appl. Phys. Lett.*, **81**, 574–576.
49. Zhao, Z., Chen, S., Shen, X., Mahtab, F., Yu, Y., Lu, P., Lam, J.W.Y., Kwok, H.S., and Tang, B.Z. (2010) Aggregation-induced emission, self-assembly, and electroluminescence of 4,4′-bis(1,2,2-triphenylvinyl)biphenyl. *Chem. Commun.*, **46**, 686–688.
50. Zhao, Z., Chen, S., Lam, J.W.Y., Chan C.Y., Chan, C.Y.K., Jim, C.K.W., Wang, Z., Wang, C., Lu, P., Kwok, H.S., Ma, Y., and Tang, B.Z. (2010) Luminescent tetraphenylethene-substituted silanes. *Pure Appl. Chem.*, **82**, 863–870.
51. Chan, L.-H., Yeh, H.-C., and Chen, C.-T. (2001) Blue light-emitting devices based on molecular glass materials of tetraphenylsilane compounds. *Adv. Mater.*, **13**, 1637–1641.
52. Chan, L.-H., Lee, R.-H., Hsieh, C.-F., Yeh, H.-C., and Chen, C.-T. (2002) Opimization of high-performance blue organic light-emitting diodes containing tetraphenylsilane molecular glass materials. *J. Am. Chem. Soc.*, **124**, 6469–6479.
53. Yuan, W.Z., Lu, P., Chen, S., Lam, J.W.Y., Wang, Z., Liu, Y., Kwok, H.S., Ma, Y., and Tang, B.Z. (2010) Aggregation-caused quenching to aggregation-induced emission: development of highly efficient emitters in the solid state. *Adv. Mater.*, **22**, 2159–2163.
54. Zhao, Z., Chen, S., Lam, J.W.Y., Lu, P., Zhong, Y., Wong, K.S., Kwok, H.S., and Tang, B.Z. (2010) Creation of highly efficient solid emitter by decorating pyrene core with AIE-active tetraphenylethene peripheries. *Chem. Commun.*, **46**, 2221–2223.
55. Zhao, Z., Chen, S., Lam, J.W.K., Wang, Z., Lu, P., Mahtab, F., Sung, H.H.Y., Williams, I.D., Ma, Y., Kwok, H.S., and Tang, B.Z. (2011) Pyrene-substituted ethenes: aggregation-enhanced excimer emission and highly efficient electroluminescence. *J. Mater. Chem.*, **21**, 7210–7216.
56. Moorth, J.N., Venkatakrishnan, P., Natarajan, P., Lin, Z., and Chow, T.J. (2010) Nondoped pure-blue OLEDs based on amorphous phenylenevinylene-functionalized twisted bimesitylenes. *J. Org. Chem.*, **75**, 2599–2609.
57. Zhao, Z., Chen, S., Lam, J.W.Y., Jim, C.K.W., Chan, C.Y.K., Wang, Z., Lu, P., Deng, C., Kwok, H.S., Ma, Y., and Tang, B.Z. (2010) Steric hindrance, electronic communication, and energy transfer in the photo- and electroluminescence process of aggregation-induced emission luminogens. *J. Phys. Chem. C*, **114**, 7963–7972.

58. Xu, B., Chi, Z., Li, H., Zhang, X., Li, X., Liu, S., Zhang, Y., and Xu, J. (2011) Synthesis and properties of aggregation-induced emission compounds containing triphenylethene and tetraphenylethene moieties. *J. Phys. Chem. C*, **115**, 17574–17581.
59. Shirota, Y. (2000) Organic materials for electronic and optoelectronic devices. *J. Mater. Chem.*, **10**, 1–25.
60. Zhang, X., Chi, Z., Xu, B., Li, H., Yang, Z., Li, X., Liu, S., Zhang, Y., and Xu, J. (2011) Synthesis of blue light emitting bis(triphenylethylene) derivatives: a case of aggregation-induced emission enhancement. *Dyes Pigments*, **89**, 56–62.
61. Liu, Y., Chen, S., Lam, J.W.Y., Lu, P., Kwok, R.T.K., Mahtab, F., Kwok, H.S., and Tang, B.Z. (2011) Tuning the electronic nature of aggregation-induced emission luminogens with enhanced hole-transporting property. *Chem. Mater.*, **23**, 2536–2544.
62. Hung, J., Yang, X., Wang, J., Zhong, C., Wang, L., Qin, J., and Li, Z. (2012) New tetraphenylethene-based efficient blue luminophors: aggregation induced emission and partially controllable emitting color. *J. Mater. Chem.* **22**, 2478–2484.
63. Zhao, Z., Chan, C.Y.K., Chen, S., Deng, C., Lam, J.W.Y., Jim, C.K.W., Hong, Y., Lu, P., Chang, Z., Chen, X., Lu, P., Kwok, H.S., Qiu, H., and Tang, B.Z. (2012) Using tetraphenylethene and carbazole to create efficient luminophores with aggregation-induced emission, high thermal stability, and good hole-transporting property. *J. Mater. Chem.*, **22**, 4527–4534.
64. Zhao, Z., Chen, S., Deng, C., Lam, J.W.Y., Chan, C.Y.K., Lu, P., Wang, Z., Hu, B., Chen, X., Lu, P., Kwok, H.S., Qiu, H., and Tang, B.Z. (2011) Construction of efficient solid emitters with conventional and AIE luminogens for blue organic light-emitting diodes. *J. Mater. Chem.*, **21**, 10949–10956.
65. Aldred, M.P., Li, C., Zhang, G.-F., Gong, W.-L., Li, A.D.Q., Dai, Y., Ma, D., and Zhu, M.-Q. (2012) Fluorescence quenching and enhancement of vitrifiable oligofluorenes end-capped with tetraphenylethene. *J. Mater. Chem.*, **22**, 7517–7528.
66. Rao, Y.-L., and Wang, S. (2011) Four-coordinate organoboron compounds with a π-conjugated chelate ligand for optoelectronic applications. *Inorg. Chem.*, **50**, 12236–12274.
67. Li, D.S., Wang, K., Hung, S., Qu, S., Liu, X., Zhu, Q., Zhang, H., and Wang, Y. (2011) Brightly fluorescent red organic solids bearing boron-bridged π-conjugated skeletons. *J. Mater. Chem.*, **21**, 15298–15304.
68. Lin, S.-L., Chan, L.-H., Lee, R.-H., Yen, M.-Y., Kuo, W.-J., Chen, C.-T., and Jeng, R.-J. (2008) Highly efficient carbazole–π-dimesitylborane bipolar fluorophores for nondoped blue organic light-emitting diodes. *Adv. Mater.*, **20**, 3947–3952.
69. Zhang, W., Chen, S., Lam, J.W.Y., Deng, C., Lu P., Sung, H.H.-Y., Williams, I.D., Kwok, H.S., Zhang, Y., and Tang, B.Z. (2011) Towards high efficiency solid emitters with aggregation-induced emission and electron-transport characteristics. *Chem. Commun.*, **47**, 11216–11218.
70. Zhao, Z., Lam, J.W.Y., and Tang, B.Z. (2012) Tetraphenylethene: a versatile AIE building block for the construction of efficient luminescent materials for organic light-emitting diodes. *J. Mater. Chem.*, **22**, 23726–23740.
71. Huang, J., Yang, X., Li, X., Chen, P. Tang, R., Li, F., Lu, P., Ma, Y., Wang, L., Qin, J., Li, Q., and Li, Z. (2012) Bipolar AIE-active luminogens comprised of an oxadiazole core and terminal TPE moieties as a new type of host for doped electroluminescence. *Chem. Commun.*, **48**, 9586–9588.
72. Lin, M.-F., Wang, L., Wong, W.-K., Cheah, K.-W., Tam, H.-L., Lee, M.-T., and Chen, C.H. (2006) Highly efficient and stable sky blue organic light-emitting devices. *Appl. Phys. Lett.*, **89**, 121913-1–121913-3.
73. Chan, C.Y.K., Zhao, Z., Lam, J.W.Y., Liu, J., Chen, S., Lu, P., Mahtab, F., Chen, X., Sung, H.H.Y., Kwok, H.S., Ma, Y., Williams, I, D., Wong, K.S., and Tang, B.Z. (2012) Efficient light emitters in the solid state: synthesis, aggregation-induced emission, electroluminescence, and sensory properties of luminogens with benzene cores and multiple triarylvinyl peripherals. *Adv. Funct. Mater.*, **22**, 378–389.
74. Zhao, Z., Chen, S., Chan, C.Y.K., Lam, J.W.Y., Jim, C.K.W., Lu, P., Chang, Z., Kwok, H.S., Qiu, H., and Tang, B.Z. (2011) A facile and versatile approach to efficient luminescent materials for applications in organic light-emitting diodes. *Chem. Asian J.*, **7**, 484–488.
75. Huang, J., Sun, N., Yang, J., Tang, R., Li, Q., Ma, D., Qin, J., and Li, Z. (2012) Benzene-cored fluorophores with TPE peripheries: facile synthesis, crystallization-induced blue-shifted emission, and efficient blue luminogens for non-doped OLEDs. *J. Mater. Chem.*, **22**, 12001–12007.

76. Chen, S., Zhao, Z., Tang, B.Z., and Kwok, H.S. (2010) Non-doped white organic light-emitting diodes based on aggregation-induced emission. *J. Phys. D*, **43**, 095101-1–095101-5.
77. Chen, S., Zhao, Z., Wang, Z., Lu, P., Gao, Z., Ma, Y., Tang, B.Z., and Kwok, H.-S. (2011) Bi-layer non-doped small-molecular white organic light-emitting diodes with high colour stability. *J. Phys. D*, **44**, 145101-1–145101-7.
78. Zhao, Z., Deng, C., Chen, S., Lam, J.W.Y., Qin, W., Lu, P., Wang, Z., Kwok, H.S., Ma, Y., Qiu, H., and Tang, B.Z. (2011) Full emission color tuning in luminogens constructed from tetraphenylethene, benzo-2,1,3-thiadiazole and thiophene building blocks. Chem. Commun., **47**, 8847–8849.
79. Li, H., Chi, Z., Zhang, X., Xu, B., Liu, S., Zhang, Y., and Xu, J. (2011) New thermally stable aggregation-induced emission enhancement compounds for non-doped red organic light-emitting diodes. *Chem. Commun.*, **47**, 11273–11275.
80. Du, X., Qi, J., Zhang, Z., Ma, D., and Wang, Z.Y. (2012) Efficient non-doped near-infrared organic light-emitting devices based on fluorophores with aggregation-induced emission enhancement. *Chem. Mater.*, **24**, 2178–2185.
81. Hosokawa, C., Eida, M., Matsuura, M., Fukuoka, K., Nakamura, H., and Kusumoto, T. (1997) Organic multi-color electroluminescence display with fine pixels. *Synth. Met.*, **91**, 3–7.
82. Huang, Y.-S., Jou, J.-H., Weng, W.-K., and Liu, J.-M. (2002) High-efficiency white organic light-emitting devices with dual doped structure. *Appl. Phys. Lett.*, **80**, 2782–2784.
83. Li, G., and Shinar, J. (2003) Combinatorial fabrication and studies of bright white organic light-emitting devices based on emission from rubrene-doped 4,4′-bis(2,2′-diphenylvinyl)-1,1′-biphenyl. *Appl. Phys. Lett.*, **83**, 5359–5361.
84. Xie, W., Wu, Z., Liu, S., and Lee, S.T. (2003) Non-doped-type white organic light-emitting devices based on yellow-emitting ultrathin 5,6,11,12-tetraphenylnaphthacene and blue-emitting 4,4′-bis(2,2′-diphenylvinyl)-1,1′-biphenyl. *J. Phys. D*, **36**, 2331–2334.
85. Xie, W., Liu, S., and Zhao, Y. (2003) A nondoped-type small molecule white organic light-emitting device. *J. Phys. D*, **36**, 1246–1248.
86. Xie, W., Hou, J., and Liu, S. (2003) Blue and white organic light-emitting diodes based on 4,4′-bis(2,2′-diphenylvinyl)-1,1′-biphenyl. *J. Phys. D*, **36**, L42–L44.
87. Yeh, S.-J., Chen, H.-Y., Wu, M.-F., Chan, L.-H., Chiang, C.-L., Yeh, H.-C., Chen, C.-T., and Lee, J.-H. (2006) All non-dopant red–green–blue composing white organic light-emitting diodes. *Org. Electron.*, **7**, 137–143.
88. Chen, S., and Kwok, H.-S. (2011) Top-emitting white organic light-emitting diodes with a color conversion cap layer. *Org. Electron.*, **12**, 677–681.
89. Wang, X.-P., Qian, Y., Zhu, T.-J., Cai, M.-M., Mi, B.-X., Jiang, X.-Y., Gao, Z.-Q., Huang, W., and Zhang, Z.-L. (2012) Non-doped white organic light-emitting diodes based on ultra-thin emitting layer with aggregation-induced emission. *Phys. Status Solidi A*, **209**, 373–377.
90. Chan, L.-H., Lee, Y.-D., and Chen, C.-T., (2006) Synthesis and characterization of 3,4-diphenylmaleimide copolymers that exhibit orange to red photoluminescence and electroluminescence. *Macromolecules*, **39**, 3262–3269.
91. Chen, H.-Y., Chen, C.-T., and Chen, C.-T. (2010) Synthesis and characterization of a new series of blue fluorescent 2,6-linked 9,10-diphenylanthrylenephenylene copolymers and their application for polymer light-emitting diodes. *Macromolecules*, **43**, 3613–3623.